ISRN LUTMDN/TMHP-19/5432-SE

ISSN 0282-1990

Simulation of solidification and cooling of a casting product using COMSOL Multiphysics

Tom Allen

Thesis for the degree of Master of Science in Engineering
Division of Heat Transfer
Department of Energy Sciences
Faculty of Engineering | Lund University

Simulation of solidification and cooling of a casting product using COMSOL Multiphysics

Tom Allen
M.Sc. Degree project in Energy Sciences
Faculty of Engineering
Lund University
April 22, 2019

This degree project for the degree of Master of Science in Engineering has been conducted at the Division of Heat Transfer, Department of Energy Sciences, Faculty of Engineering, Lund University, and at RISE Swecast.
Supervisor at the Division of Heat Transfer was Professor Bengt Sundén.
Supervisor at RISE Swecast was Dr Raul Carlson.
Examiner at Lund University was Dr Zan Wu.

The project was carried out in cooperation with Karlstad Foundry, a part of Valmet.

Thesis for the Degree of Master of Science in Engineering

ISRN LUTMDN/TMHP-19/5432-SE

ISSN 0282-1990

Division of Heat Transfer
Department of Energy Sciences
Faculty of Engineering, Lund University
Box 118, 221 00 Lund
Sweden

www.energy.lth.se

ACKNOWLEDGEMENTS

I want to thank everyone who has been a part of the work with this project. Thank you to Prof. Bengt Sundén and Associate Professor Zan Wu at the Division of Heat Transfer, who have contributed with valuable comments about the work since the start. Thank you to Dr Raul Carson, who has been supervisor at RISE Swecast, for your ideas, your challenging questions about the results, and not the least your encouragement throughout all the difficulties during the project.

Thank you Christoffer Fransson at Valmet Foundry in Karlstad who has contributed with a lot of materials regarding the casting procedure and technical details. Also, thank you Rolf Jonsson at Valmet, who hosted a study visit at the foundry together with Christoffer.

I would also like to thank COMSOL Support in general, and Magnus Björkman in particular, who have contributed a lot with help regarding building and simulating the model. Thank you Anton Löfgren, who always had his door and mailbox open for questions about COMSOL, and thank you Tove Rappmann who has proof read the report.

At last, thank you to my mother Beata, for keeping me going whith the project when things has been quite tough. Du hade rätt som vanligt, det löser sig till slut.

ABSTRACT

In this project, the cooling and solidification processes for a Valmet Foundry product have been simulated in order to shorten the cooling time. The study has also been done in cooperation with RISE Swecast in Jönköping, as a part of finding ways to make casting procedures more energy efficient. Another scope of the study is to evaluate how well COMSOL Multiphysics can be used to simulate these types of casting processes.

A large part of the study has been about the simulation, but some information regarding material properties and process temperatures have been collected from RISE Swecast and Valmet. The model in COMSOL Multiphysics is based on a CAD file describing the casting product, and the surrounding sand form has been built around it as a part of the modeling.

Initially, the current process was modeled and simulated to get the model to work as close to reality as possible. When the model describing the current case was deemed to be close enough to reality, some changes of the casting form were tested. The conductivity in the form was increased using metal fins, and a forced air stream was introduced to increase the convective heat flux of the sand form.

The results of the studies shows that the cooling fins and air stream do not affect the cooling time notably by themselves, but combined they could make quite a big difference for the cooling process. The fins increase the turbulence of the introduced air flow which improves the convective heat transfer, and the cold air stream works as a heat sink for the fins.

COMSOL Multiphysics is found to be an efficient way to model this type of procedures because of the way different physical concepts can be coupled, in this case heat transfer and turbulent air flow. It is also convenient to work with important CAD models in the program, and to model the phase change in a material. However, it demands a lot of knowledge about both the physics and how to build an effective mesh to get the most of the simulations.

Keywords: heat transfer, casting, phase change, COMSOL Multiphysics

SAMMANFATTNING

Detta projekt har gått ut på att simulera stelnings- och avsvalningsprocessen för ett gjutgods i COMSOL Multiphysics, med syfte att förkorta avsvalningstiden för produkten. Gjutgodset produceras för Valmet på Karlstad Gjuteri. Projektet har också genomförts tillsammans med RISE Swecast i Jönköping med syftet att hitta sätt att få gjuteriprocesser mer energieffektiva. Ett annat syfte med studien har varit att utvärdera COMSOL Multiphysics som ett verktyg för att simulera denna typ av processer.

Projektet har till stor del utgjorts av modellering och simuleringen av modellen, och viss information rörande materialspecifikationer och temperaturer i processen har hämtats in från RISE Swecast och Valmet. Modellen som används i simuleringen bygger på en CAD-fil föreställande gjutgodset, och den omgivande sandformen har byggts runt den i COMSOL som en del av modelleringen.

Den första delen av projektet var att modellera och simulera den nuvarane processen så att den stämde så väl överens med verkligheten som möjligt. När modellen ansågs vara tillräckligt nära verklighen modifireades den för att testa ett par förändringar av formen. Värmeledningen i sandformen ökades genom att bygga in metallfenor, och ett luftflöde leddes genom formens ihålighet för att öka värmekonvektionen.

Studiens resultat visar att när kylfenorna eller luftströmmen används påverkas inte slutresultatet nämnvärt, men när de två metoderna kombineras kan det medföra en betydande skillnad för processen. Fenorna bidrar till en ökad turbulens i luftkanalen vilket ökar konvektionen. Samtidigt agerar luftströmmen som en kylning för metallfenorna.

I studien anses COMSOL Multiphysics vara ett effektivt verktyg för att modellera denna typ av processer, främst på grund av hur enkelt olika fysikmoduler kan kopplas till varandra, i detta fall värmeöverföring och turbulens. Det är också smidigt att jobba med importerade CAD-modeller i programmet, samt att simulera fasövergångar. En potentiell baksida med att använda programmet är att det kräver mycket av användaren avseende teorin bakom de fysiska fenomenen samt modelleringsfärdigheter för att få ut det mesta av simuleringarna.

Nyckelord: värmeöverföring, gjutgods, fasövergång, COMSOL Multiphysics, modellering, simulering

ABBREVIATIONS

α	Thermal expansion coefficient
ε	Dissipation of turbulent kinetic energy
κ_V	von Kárman constant
λ	Thermal conductivity (W/m/K)
ρ	Density (kg/m^3)
c_p	Specific heat (kJ/kg/K)
H	Enthalpy (kJ/kg)
h	Overall heat transfer coefficient (W/m^2/K)
I_T	Turbulence intensity
k	Heating coefficient (W/m^3/K)
k	Turbulent kinetic energy
L_T	Turbulence length scale (m)
$\mathbf{n}$	Normal vector towards exterior
Q	Heat source (W/m^3)
$\mathbf{q}$	Conductive heat flux (W/m^2)
Q_0	Distributed heat source (W/m^3)
q_0	Inward heat flux (W/m^2)
Q_p	Pressure work (W/m^3)
Q_{vd}	Viscous dissipation (W/m^3)
T	Temperature (°C)
t	Time (h)
T_{ext}	External temperature (°C)
$\mathbf{u}$	Velocity (m/s)
U_0	Normal inlet velocity (m/s)
U_{ref}	Reference velocity scale (m/s)

Contents

1 Introduction

1.1 Context and challenges

In a society where energy efficiency is getting more important due to resource limitations and emissions, it is in multiple actors interest to see how different types of energy demanding processes can be changed to the better. One of the most energy demanding industries in Sweden is the iron, steel and metals-industries, which accounted for 15% of the total energy consumption in Sweden 2015 (Energimyndigheten, 2017). For the industries themselves, there could be an interest to enhance the resource efficiency for economic reasons.

For this project, RISE Swecast in Jönköping and Valmet Foundry in Karlstad wanted to investigate possibilities to change the cooling of one of the casting products in order to make it more efficient. The benefit for Valmet would be to shorten the residence time for the product, which would allow a higher production rate for the industry[1]. One of the goals with this type of investigations for RISE Swecast is to find ways to better make use of heat that in today's industry is an energy loss.

1.2 Objectives

The objective of this master thesis project has been to simulate the heat transfer in an iron casting form, and to increase the cooling rate of the casting. By extension, the objective has also been to investigate the possibilities to reuse the heat from the casting in some way. This study, however, is limited to the casting form itself and possible air inlets and outlets. How or for what the excess heat could be used is not a part of the study.

Another objective of the project has been to investigate how this kind of casting processes can be modeled and simulated using COMSOL Multiphysics.

1.2.1 Problem statements

For the project, two main problem statements have been chosen for evaluation.

- What are some efficient ways to decrease the cooling time for a casting product at Valmet Foundry?
- How can a sand casting procedure be modeled using COMSOL Multiphysics?

For the first problem statement, the study aims to investigate different ways to model and simulate the cooling, and how the simulated cases could be

[1] Visit at Valmet Foundry in Karlstad, 12/9 2018.

implemented in the real production. For the second problem statement, some of the advantages and disadvantages of using COMSOL Multiphysics for this type of processes should be found.

2 Theory

2.1 The casting process

At Valmets foundry in Karlstad, the casting procedure is performed in sand forms. The casting forms are built in sand from a model, and the sand keeps the shape by introducing a binding material. When the form is done, the molten iron is poured into the sand form where it solidifies and cools down. When the casting is cool enough, the sand form is cracked and the casting is extracted from the form.[2]

The sand used in the forms at Valmet is a mix between Baskarp B45 and chromite. The B45 in turn consists of 80% quartz and 20 % feldspar, and the amount of chromite in the sand at Valmet is very low. Figure 1 shows the thermal conductivity for different types of sand which uses water and betonite as a binder(Farre, 2012).

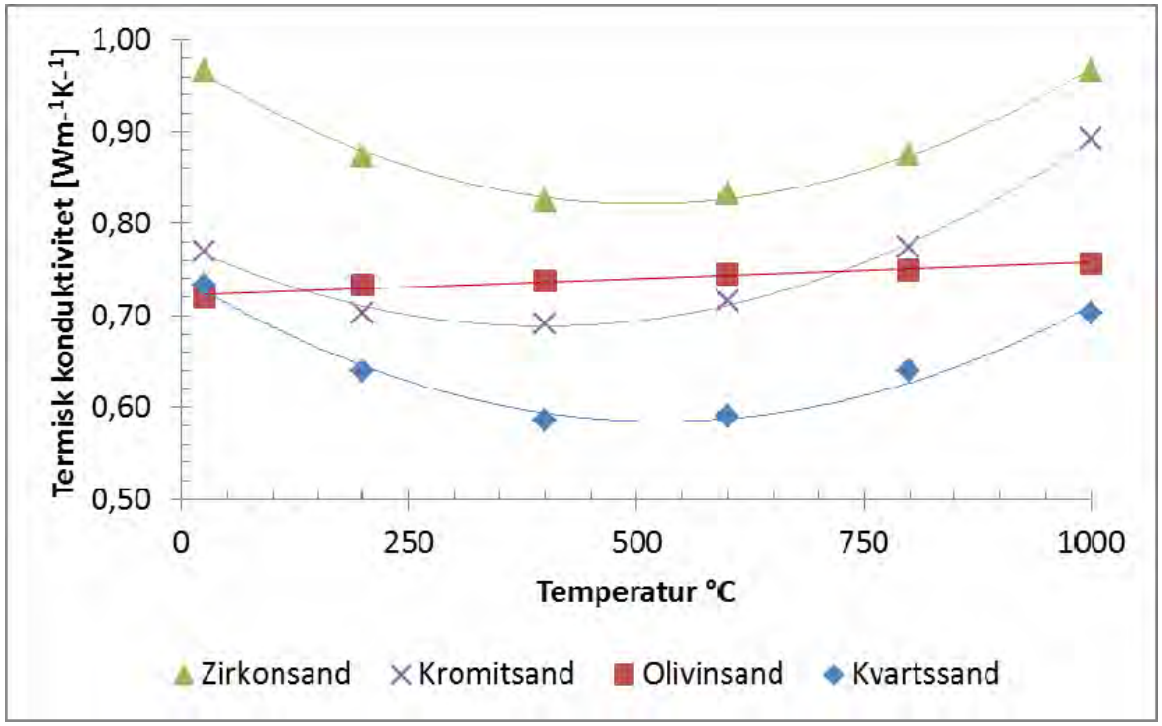

Figure 1: Thermal conductivity against temperature for different kinds of sand which use water and betonite as binder. "Kvartssand" (quartz sand) is the sand mainly used for this model (Farre, 2012).

The binding material used at Valmet is a furan binder. It is a mix between furan alcohol and phosphorus/PTS acid, where the acids are used for polymerization of the furan alcohol[3]. It is worth noting that the conductivity in the sand is affected by the choice of binder, and that furan binder contributes to a lower thermal

[2]Visit at Valmet Foundry in Karlstad, 12/9 2018.
[3]Mail correspondence with Mahsa Saeidpour, RISE Swecast, 18/12 2018.

conductivity than water and betonite does (Farre, 2012). Except for the sand, the form also consists of 24 cooling blocks. These are quite large iron parts, and the purpose of them is to increase the heat rate in the form.

Valmet has provided information regarding the casting procedure. When the liquid iron is poured into the sand form, it has a temperature of 1200 °C. The mass of the casting iron product is 23 tonnes [4]. After five days, when the casting product is removed from the sand form, the maximum temperature in the casting is 450 °C. During the solidification and cooling processes, the sand form stands exposed to the open air, which can be assumed to stand still and be at 25 °C[5].

2.2 Physical concepts

2.2.1 Heat transfer

The heat transfer phenomena in the casting process are modeled in two different ways depending on the phase of the material (i.e, if the material is in a solid or liquid state). In the model, the sand form is modeled as a solid and the air as a fluid throughout the whole simulation. The cast iron is initially modeled as a fluid, but as it cools down it turns into a solid (see *2.2.2 Phase change*).

Solids

The solid parts of the model are the sand and the casting itself after solidification. The heat transfer process for the solid parts in the model is defined according to Eq. 1 (COMSOL, 2018c).

$$\rho c_p \left(\frac{\partial T}{\partial t} + \mathbf{u_{trans}} \cdot \nabla \mathbf{T} \right) + \nabla \cdot (\mathbf{q} + \mathbf{q_r}) = -\alpha T : \frac{\partial S}{\partial T} + Q \tag{1}$$

Using Fourier's heat conduction law (Sundén, 2012), the heat transfer due to conduction $\mathbf{q}$ is defined as Eq. 2.

$$\mathbf{q} = -\lambda \nabla T \tag{2}$$

Since the solid parts are not moving, $\mathbf{u_{trans}} = 0$ in Eq. 1. The volume is assumed to be constant, making the derivative of the stress tensor S equal to zero. The model does not take account for any thermal radiation, which makes $\mathbf{q_r} = \mathbf{0}$. With regards to these assumptions and Eq. 2, Eq. 1 can be rewritten with the internal energy change in time on the left hand side, and the heat transfer in space on the right hand side according to Eq. 3 .

$$\rho c_p \frac{\partial T}{\partial t} = \lambda \nabla^2 T + Q \tag{3}$$

[4] Visit at Valmet Foundry in Karlstad, 12/9 2018.

[5] Mail correspondence with Christoffer Fransson, Production Technique & Quality Manager at Valmet, 10/12 2018.

The specific heat c_p in the casting iron is determined based on data provided by RISE Swecast. The data, which is presented in Appendix, shows how the specific enthalpy h is dependent of the temperature T. The data points are used to perform a linear regression, and the expressions obtained are used to determine the specific heat according to Eq. 4 (Spakovszky, 2007).

$$c_p = \left(\frac{\partial h}{\partial T}\right)_p \tag{4}$$

Note that this correlation is valid under the assumption that there is no pressure change in the substance.

Fluids

The heat transfer in the fluid module is used in the air channel and in the casting during the phase change. COMSOL defines the heat transfer process in fluids according to Eq. 5 (COMSOL, 2018c).

$$\rho C_p \left(\frac{\partial T}{\partial t} + \mathbf{u} \cdot \nabla T\right) + \nabla \cdot \mathbf{q} = \alpha_p T \left(\frac{\partial p}{\partial t} + \mathbf{u} \cdot \nabla p\right) + \tau : \nabla \mathbf{u} + Q \tag{5}$$

In the air channel, the velocity $\mathbf{u}$ is determined by the turbulent flow module, described in *2.2.3 Turbulent flow*. As in the solid case, $\mathbf{q}$ can be expressed using Eq. 2. α_p is the coefficient of thermal expansion and τ is the viscous stress tensor. Since all material used in the model is considered as incompressible and the pressure is assumed constant, the stress tensors and thermal expansions can be neglected. Rearanging Eq. 5 by putting the heat change in time on the left hand side and the heat change in space on the right hand side, 6 is obtained.

$$\rho C_p \frac{\partial T}{\partial t} = \lambda \nabla^2 T - \rho C_p \mathbf{u} \nabla T + Q \tag{6}$$

2.2.2 Phase change

The solidification of a single material occurs at a specific temperature. However, this is not the case in castings since the material used often is a mix of different components. Instead, the phase change occurs over a temperature interval. This interval is limited by the liquidus and solidus temperatures, or T_L and T_S, respectively (Askeland and Wright, 2017). In this interval, some of the material properties can be determined using the *apparent heat capacity method*. This method uses the fraction of material in liquid state, expressed as the smoothed function $\theta\,(T)$, and the material properties for the solid and liquid phases to get a weighted mean value for the casting (Bannach, 2014). θ is shown in Fig. 2, where θ_1 is equal to θ and θ_2 is equal to $1-\theta$. The interval $\Delta T_{1\to 2}$ is limited by T_L and T_S, and $T_{pc,1\to 2}$ is the mean value of T_L and T_S (Bannach, 2014).

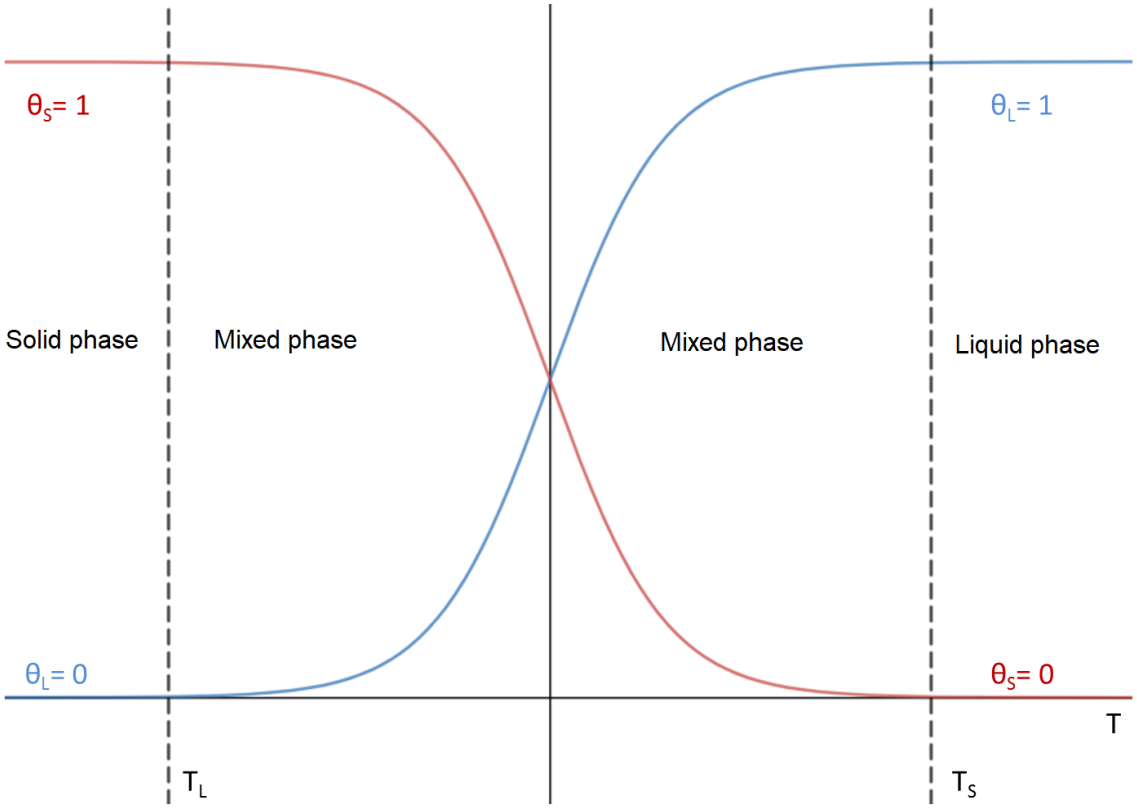

Figure 2: The function $\theta\,(T)$ that COMSOL uses during the phase change.

In COMSOL, the phase transition of the casting is a sub node to the heat transfer module. The $\theta\,(T)$ function is used by COMSOL to determine the specific heat, themal conductivity and density during the phase change according to Eqs. 7-9.

$$c_p = \frac{1}{\rho}\left(\theta_1 \rho_{ph1} c_{p,ph1} + \theta_2 \rho_{ph2} c_{p,ph2}\right) + c_L \tag{7}$$

$$\lambda = \theta_1 \lambda_{ph1} + \theta_2 \lambda_{ph2} \tag{8}$$

$$\rho = \theta_1 \rho_{ph1} + \theta_2 \rho_{ph2} \tag{9}$$

Since the density of the iron is assumed to be constant due to the constant volume and conservation of mass, $\rho_{ph1} = \rho_{ph2} = \rho$.

c_L in Eq. 7 represents the *latent heat distribution*, which is the specific heat released from the casting due to the phase transition. The latent heat distribution is approximated in COMSOL as Eq. 10 (COMSOL, 2018c).

$$c_L\,(T) = L\frac{d\alpha_m}{dT} \tag{10}$$

L denotes the *latent heat of melting*, and α_m is the mass fraction of the liquid phase during the phase transition. α_m is dependent of θ as described by Eq. 11.

$$\alpha_m = \frac{1}{2}\frac{\theta_2\rho_{ph2} - \theta_1\rho_{ph1}}{\rho} \tag{11}$$

Material parameters provided by RISE Swecast regarding the phase change are presented in Table 1.

Table 1: Phase change parameters for the casting iron.

Parameter	Value
T_L	1202 °C
T_S	1137 °C
L	282.2 kJ/kg

2.2.3 Turbulent flow

The temperature change in the casting is not only dependent on the heat transfer in each material, but also by the air flux in the middle of the stream. The movement of a fluid such as air can be modeled as either a laminar or a turbulent flow. In this project, the air flow has been modeled as turbulent.

Modeling turbulent flow demands a lot of computational power, especially when modeled in 3D. The model simulates the turbulent flow with a *Reynolds Average Navier-Stokes* (RANS) procedure. This means that instead of simulating all velocity fluctuations in the air stream, the model calculates an average velocity $\overline{\mathbf{v}}$. In order to simulate the turbulence in the air channel, the k-ε model is used. The turbulence is approximated with the properties k and ε, which represent the turbulent kinetic energy and the rate of dissipation of turbulent energy, respectively. The flow in the Turbulence flow node is modeled according to Eq. 12-13 (Nilsson, 2017).

$$\rho\frac{\partial\overline{\mathbf{v}}}{\partial t} = -\rho\overline{\mathbf{v}}\cdot\nabla\overline{\mathbf{v}} - \nabla\overline{p} + \rho\mathbf{g} + \nabla\left(\mu+\mu_T\right)\cdot\nabla\overline{\mathbf{v}} - \rho\frac{2}{3}\nabla k \tag{12}$$

$$\nabla\cdot\overline{\mathbf{u}} = 0 \tag{13}$$

The properties k and ε are defined according to Eqs. 14 - 17, where μ_T represents the turbulent viscosity (Nilsson, 2017).

$$\rho\frac{\partial k}{\partial t} = -\rho\overline{\mathbf{v}}\cdot\nabla k + \nabla\cdot\left(\left(\mu+\frac{\mu_T}{\sigma_k}\right)\nabla k\right) + P_k - \rho\varepsilon \tag{14}$$

$$\rho\frac{\partial\varepsilon}{\partial t} = -\rho\overline{\mathbf{v}}\cdot\nabla\varepsilon + \nabla\cdot\left(\left(\mu+\frac{\mu_T}{\sigma_\varepsilon}\right)\nabla\varepsilon\right) + C_{\varepsilon1}\frac{\varepsilon}{k}P_k - C_{\varepsilon2}\rho\frac{\varepsilon^2}{k} \tag{15}$$

$$P_k = \mu_T\left(\nabla\overline{\mathbf{v}} : \left(\nabla\overline{\mathbf{v}} + \left(\nabla\overline{\mathbf{v}}\right)^T\right) - \frac{2}{3}\left(\nabla\cdot\overline{\mathbf{v}}\right)^2\right) - \frac{2}{3}\rho k\nabla\cdot\overline{\mathbf{v}} \tag{16}$$

$$\mu_T = \rho C_\mu \frac{k^2}{\varepsilon} \tag{17}$$

The equations above are based on a number of fixed constants, which are presented in Table 2 (Nilsson, 2017).

Table 2: Constant parameters for the k-ε-model (Nilsson, 2017).

Parameter	Value
C_μ	0.09
$C_{\varepsilon 1}$	1.44
$C_{\varepsilon 2}$	1.92
σ_k	1.0
σ_ε	1.3

The consequence of Eq. 13 is that the air is modeled as an incompressible fluid with a constant density, which in turn indicates that convective heat transfer due to air movement caused by temperature differences is not taken account of. This problem is solved when the CFD module is coupled with the heat transfer module.

2.2.4 Physics coupling

To get the heat transfer model and the CFD model to be co-dependent, the two physics interfaces has to be coupled with each other. In COMSOL, this is achieved by using the built in multiphysics node *Nonisothermal flow*. This node is only applicable on the parts of the model that uses both of the physics interfaces described above, in this case the air channel, and combines the equations for heat and mass transfer to evaluate the temperature and velocity of the air in the selected part (COMSOL, 2018c).

As stated by Eq. 13, the air is assumed to be incompressible by the CFD module itself. However, to simulate the natural convection due to density changes in the air, Boussinesq approximation is used. The approximation uses the reference density ρ_0 at a given temperature T_0, and assumes that the density can be expressed as Eq. 18 (COMSOL, 2018a).

$$\rho = \rho_0 \left(1 - \alpha \left(T_0\right) \left(T - T_0\right)\right) \tag{18}$$

The air movement could also be modeled by defining the air as a compressible or weakly compressible fluid. However, using Boussinesq approximation to model the natural convection makes the calculations simpler, thus reducing the computational time for the simulation (Fontes, 2016). The Boussinesq approximation is only used inside the air channel, and when there is no forced air

flow. In the cases of a forced air flow, the heat transfer due to natural convection is assumed to be negligible [6].

[6] Correspondence with Magnus Björkman, COMSOL Support, 28/2 2019.

3 Method & work procedure

The project has mainly been performed as a simulation study, with COMSOL Multiphysics as the simulation tool. Model specific data, such as CAD files and material properties, have been collected from Valmet in Karlstad and RISE Swecast in Jönköping.

3.1 Simulations with COMSOL Multiphysics

COMSOL Multiphysics was chosen as the simulation tool because of the opportunities to couple heat and mass transfer phenomena to each other (as described in chapter 2.2.4), and the ability to import a CAD file in a convenient way. The backside of using COMSOL could be that there is other software that is more applicable for casting simulations.

One of the important factors when modeling with COMSOL Multiphysics is deciding the mesh for the model. The mesh is the grid which determines how many data points will be evaluated in the model. A finer mesh implies more data points, thus increasing the calculations and computational time required to solve the problem. However, a model that has too coarse mesh will not represent the geometry well, and could affect the results of the simulation. If the CAD model has, for example, too narrow faces or edges for the mesh to handle, COMSOL will notify the user of this as a warning. The model could still be ”simulateable”, but it is recommended to either change the mesh size to a finer or simplifying the geometry if this happens (Gothäll, 2017).

3.2 Data collection

The material data that has been used in simulations was initially based on reports and data from RISE Swecast, and has been modified in order to get results close to reality. Some of the data has also been collected from Valmet, who is the manufacturer of the casting product. The used data and the modifications performed on the data are described in chapter 4.1.2.

3.3 Application for Valmet

A CAD model describing the casting product was provided by Valmet, and has made up the backbone for the building of the sand form in COMSOL. Valmet also provided a CAD assembly file describing the casting product as well as the other components in the form. The assembly file has been used as a reference model for the simplified geometry built for this project. However, the provided assembly file has not been used for the simulation due to the complex geometry.

A major difference between the model and the real sand form is the cooling blocks, which are not explicitly built in the model. Instead, the conductivity of the sand form as a whole is determined via trial and error-simulations. This has been done due to time limitations in the project.

Another difference between the model and the real process is the sand saving ”skeleton” that Valmet uses. In the model, there is nothing between the air channel and the sand. However, in reality there is an iron pipe that forms a ”layer” between them. The pipe has been neglected in the reality because of the narrow thickness of the pipe. COMSOL needs to use a finer mesh in order to incorporate the pipe in the modeling, which increased the computational time drastically. The air channel itself is modeled with a diameter of 0.8 m. However, the real life application has a diameter of 1 m. This is due to a reading error of the drawing, and was found too late in the project to be considered.

4 Modeling & simulation

4.1 Reality & Model

4.1.1 Geometry

Initially, a 2D axi-symmetric model was tried to build in order to describe the process. This was not successful because the casting flask has a quadratic bottom area, making it impossible to recreate geometrically in that way. The model was instead built as a 3D component, which made it possible to use CAD-files of the components provided by Valmet. The CAD-file used was slightly simplified by merging some smaller faces, and used to build the surrounding sand form. In order to decrease the computational time for the simulation, some symmetry advantages are used to only model one quarter of the model. Figure 3 shows the 3D-models used in the simulations. In the simulations where a forced air flow has been introduced in the model, the air channel shown in Figure 3c has been expanded "downwards".

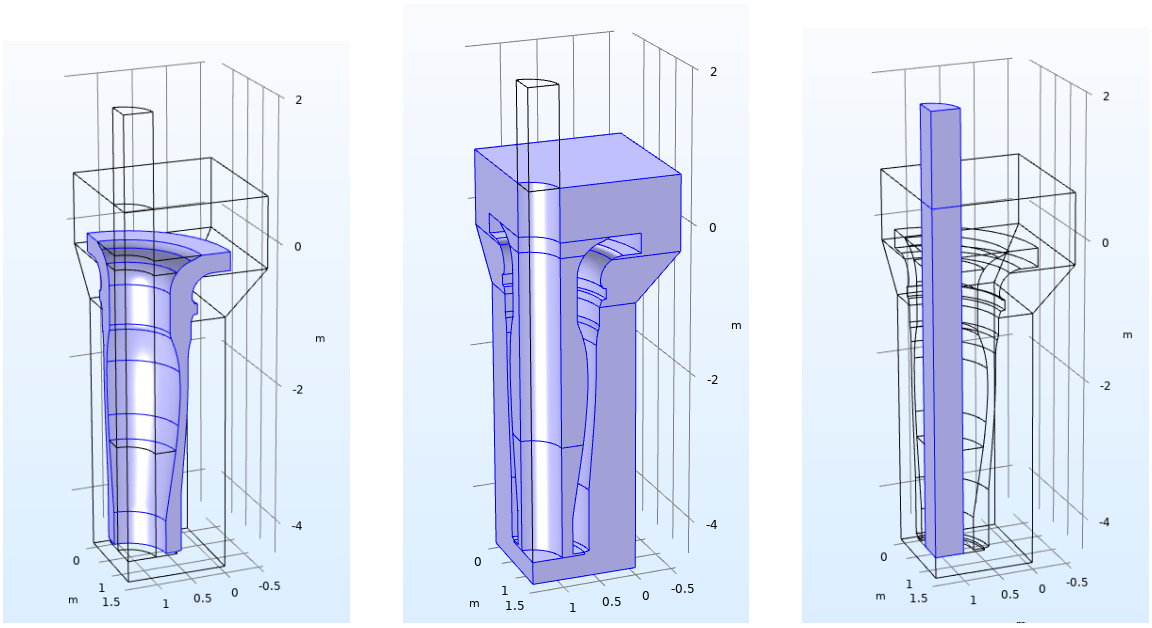

(a) The casting product. **(b)** The sand form. **(c)** The air channel

Figure 3: The (quartered) geometry used in the simulations.

Initially, the cooling blocks mentioned in section 2 Theory was included in the model. However, when the conductivity for the sand was determined, the cooling process without the blocks gave a result that matched the real temperature profile in the casting. When the cooling blocks were present in the model, the heat conductivity for the sand had to be very low to avoid the casting to get to cold after 120 h. This, and simplifying the geometry to shorten the computational time, motivated further modeling without the cooling blocks.

4.1.2 Equations, assumptions and simplifications

The equations used when setting up the model is described under *2 Theory*. The thermal conductivity λ and the specific heat c_p for the casting iron was determined from experimental data from RISE Swecast (presented in Appendix A). The data points where used to make linear regressions over two different temperature intervals. One of the regressions consider the liquid state of the material, and the other consider the solid ditto. In order to reduce computational time, the results from the regressions where used to find a mean value for the solid and liquid phase, respectively. Those parameters are presented in Table 3. Since the pressure in the casting is assumed to be constant, the heat capacity of the iron has been determined from the specific heat according to Eq. 4. The specific heat has been determined for the solid and liquid phase separately.

The density for the casting iron is determined from the volume of the CAD file from Valmet and the mass of the iron used in the production. The model does not take any change in volume into account. Therefore, the density is modeled as a constant, temperature independent parameter due to conservation of mass.

The heat capacity and conductivity for sand have been determined using data from Swecast (Farre, 2012). For computational reasons, the conductivity has been approximated with a constant value, and modified to give a result that fits with reality ($T_{max}\,(120h) \approx 450$ °C). After some trial and error-simulations, $\lambda_{sand} = 0.45$ W/m/K and $c_{p,sand} = 1000$ kJ/kg was deemed realistic.

All properties for the materials, except air, used in the model are presented in Table 3. The data concerning air is taken from COMSOLs material data base (COMSOL, 2018b).

Table 3: Material parameters used in the simulation.

Material	$\lambda\,[W/m/K]$	$c_p\,[J/kg/K]$	$\rho\,[kg/m^3]$
Cast iron (liquid)	31	831.2	4792
Cast iron (solid)	25	585.8	4792
Sand	0.5	1000	1630

4.1.3 Initial values

Ideally, the model should be set with two different initial temperatures; one for the casting at 1200 °C and one for the rest of the components at 25 °C. However, that approach came with some complications regarding the convergence of the problem in Comsol. Therefore, the initial value was set to 25 °C everywhere in the model and a *distributed heat source* Q_0 was used to heat the casting, defined by Eq. 19.

$$Q_0 = (T_{control} - T) \cdot k \cdot (\theta\,(0) - \theta\,(\tau)) \tag{19}$$

Here, $T_{control}$ puts a maximum temperature for the heating process, k determines the "speed" of the heating, and τ is the time the heat source is active. The function $\theta(t)$ is the step function, and works as a "switch" for the heat source. When $t > \tau$, the whole expression is equal to 0. For this case, $\tau = 330s$, which is the time it takes to pour the molten iron into the sand form. A variety of different values for $T_{control}$ and k were tested to find fitting values. The following criteria were used in the decision.

- the mean temperature should be as close to 1200 °C as possible,
- virtually all of the casting iron should be in liquid state at $t = \tau$,
- the total amount of added energy from the heat source should be close to the heat theoretically needed to heat the iron from 25 °C to 1200 °C.

In order to determine how well the model follows the last criterion, the energy required theoretically was calculated from the enthalpy data in Appendix A according to Eq. 20.

$$\Delta E_{theoretical} = \Delta(hT) \cdot m \tag{20}$$

A variety of parameters for Eq. 19 was then tested, and for each test Q_0 was integrated as a Riemann sum for each time step taken by COMSOL from t=0 s to t=330 s ($\Delta E_{simulation}$). The latter energy term was then divided with the theoretical energy demand to see how well they matched. The parameters chosen for the model is presented in table 4. Figure 4 shows the heat source behaviour for

Table 4: Parameters used for the heating process

Parameter	**Value**
$T_{control}$	$1300\ °C$
k	$43 \cdot 10^3\ W/m^3/K$

t=0 until t=360 s. When evaluated as described above, the fraction between $\Delta E_{simulation}$ and $\Delta E_{theoretical}$ is 1.11. The calculations with these parameters are presented in Appendix B.

The initial air velocity is set to 0 m/s in all directions.

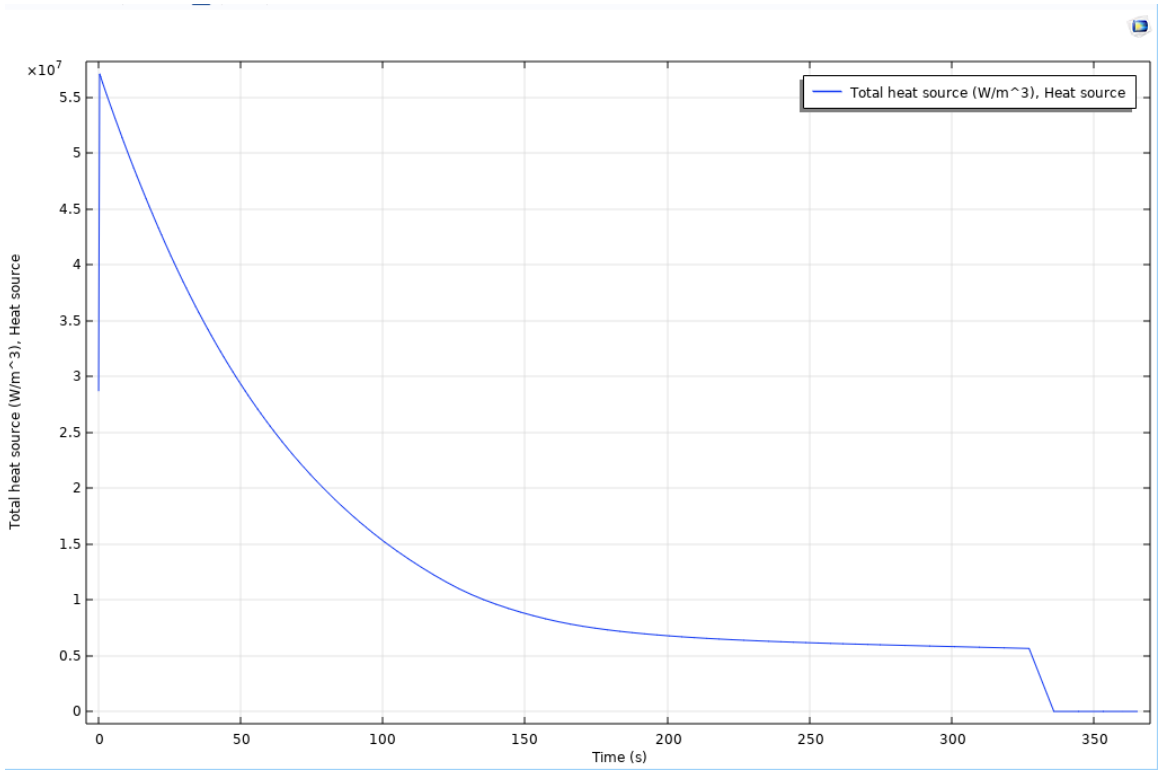

Figure 4: Power generated from the heat source.

4.1.4 Boundary conditions

Heat transfer

The heat transfer model requires boundary conditions along the outer borders of the sand form and the chimney part of the air channel. At the border between sand and air, natural convection is assumed to occur. This is modeled with a heat transfer coefficient h related to the heat flux q over the border according to Eq. 21. Here, $h = 3$ W/m^2/K was assumed to be a good standard value[7].

$$q_0 = h\,(T - T_{ext}) \tag{21}$$

At the top of the air channel, the boundary is modeled as an open boundary (Eq. 22), where $\mathbf{n}$ is the normal vector towards the exterior. The open boundary condition means that if the air moves into the channel, the boundary is treated as an Dirichlet boundary condition. If the air moves out of the channel, the conductive heat flux into the channel is 0.

$$\begin{cases} T = T_{ext}, & \text{if } \mathbf{n}\cdot\mathbf{u} < 0 \\ -\mathbf{n}\cdot\mathbf{q} = 0, & \text{if } \mathbf{n}\cdot\mathbf{u} \geq 0 \end{cases} \tag{22}$$

[7]Meeting with Bengt Sundén, Professor Emeritus at the division of Heat Transfer at Lund University, 22/1 2019

Since only one quarter of the full casting is simulated, a symmetry boundary condition is applied at the surfaces where the model was cut. The temperatures at both sides of the symmetry line are equal to each other, which implies that there is no temperature gradient driving the conductive heat flux. Therefore, the heat flux over the symmetry line is 0, as shown by Eq. 23.

$$-\mathbf{n}\cdot\mathbf{q}=0 \tag{23}$$

The face facing down is assumed to be in direct contact with a low-conductive material, motivating a thermal insulation boundary condition at that location. The same boundary condition is applied for the walls of the "chimney" of the air channel for numerical reasons. Since thermal insulation implies that there is no heat flux over the boundary, Eq. 23 is valid for this boundary condition as well.

Turbulent flow

The turbulent flow model requires boundary conditions around the air channel. The top of the channel is, just like in the heat transfer model, equipped with an open boundary condition. This sets the pressure at the boundary to the sum of a given normal stress f_0 and the hydro-static pressure p_{hydro}. Since the model works with relative pressure and the air channel is open to the surrounding air, $f_0 = 0$. The hydro-static pressure is dependent on the height of the model

$$\begin{cases} p_{hydro} = \rho_{ref}\mathbf{g}\cdot(\mathbf{r}-\mathbf{r}_{ref}) & \text{for all cases} \\ \nabla k\cdot\mathbf{n}=0, \nabla\varepsilon\cdot\mathbf{n}=0 & \text{if } \mathbf{u}\cdot\mathbf{n}\geq 0 \\ k=\frac{3}{2}\left(U_{ref}I_T\right)^2, \varepsilon=\frac{C_\mu^{3/4}k^{3/2}}{L_T} & \text{if } \mathbf{u}\cdot\mathbf{n}<0 \end{cases} \tag{24}$$

For an open boundary, $U_{ref} = 1$ m/s, $I_T = 0.005$ and $L_T = 0.1$ m (COMSOL, 2018a). $\mathbf{r}$ is the height at which the open boundary is, and r_{ref} is the reference height (in this case 0). C_μ is a turbulence constant presented in Table 2.

The boundary between the air and the sand is modeled as a wall, which gives a Dirichlet boundary condition for the velocity according to Eq. 25. This is also the case for the walls of the "chimney" of the air channel. COMSOL uses *Wall functions* close to the walls . The *k*-ε-model is not valid close to walls, and for computational reasons COMSOL uses analytical functions to describe the dissipation of turbulence in those areas (Frei, 2017). The boundary condition at the wall is described by Eq. 25.

$$\begin{cases} \mathbf{u}\cdot\mathbf{n} &= 0 \\ \nabla\cdot k &= 0 \\ \varepsilon &= \frac{C_\mu^{3/4}k^{3/2}}{\kappa_v\delta_w} \end{cases} \tag{25}$$

κ_v is the Von Kárman constant (set by default to 0.41) and δ_w is the wall lift-off, i.e. the distance from the wall which the analytical calculation is performed within.

As in the heat transfer model, a symmetry boundary condition is applied at the cut surfaces. All driving forces are assumed to be equal at the symmetry line, making the gradients for velocity, turbulence kinetic energy and dissipation of turbulence zero, as described by Eq. 26.

$$\begin{cases} \mathbf{u} \cdot \mathbf{n} & = 0 \\ \nabla k \cdot \mathbf{n} & = 0 \\ \nabla \cdot \varepsilon & = 0 \end{cases} \tag{26}$$

In the cases of forced convection, the inlet boundary is set with a normal inlet velocity U_0, and the outlet has a reference pressure of $p_{ref} = 0$.

4.2 Mesh

In COMSOL, the mesh of a model can either be modeled manually by the user, or automatic by the program. When meshing with the automatic mesh feature, the mesh size needs to be defined by the user. The scale goes from ”extremely coarse” to ”extremely fine”. A coarser mesh will generate fewer mesh elements, which demands fewer calculations but could also represent the model geometry in an insufficient way. On the other hand, a finer mesh will generate a more representative meshing structure, but at the cost of an increased computational time. This links with the mesh Independence, i.e., the simulation results should not be dependent on the meshing structure. COMSOLs automatic mesh generator increases the number of mesh elements in ”critic” areas of the model to avoid this problem, and as stated in 3.1 *Simulations with COMSOL Multiphysics*, the program notifies the user if the selected mesh size is to coarse to represent the geometry in a sufficient way.

4.3 Simulation

The first thing that happens when the simulation starts is the heating of the cast iron for 330 s, as described by Eq. 19. The average, maximum and minimum temperatures in the casting are shown in Fig. 5. Figure 6 shows the phase indicator distribution for the solid phase at t=330 s, where the dark blue area represents material in more or less liquid state. The heating procedure is assumed to be the same for all of the different cases. The results from the cooling are however dependent of how the different model setups look. The simulation results are therefore presented in sections 4.4-4.7. It is worth noting that if nothing else is stated, all velocity and temperature profiles are projected on a ”cut plane” from the center line of the air channel to the corner of the sand casting.

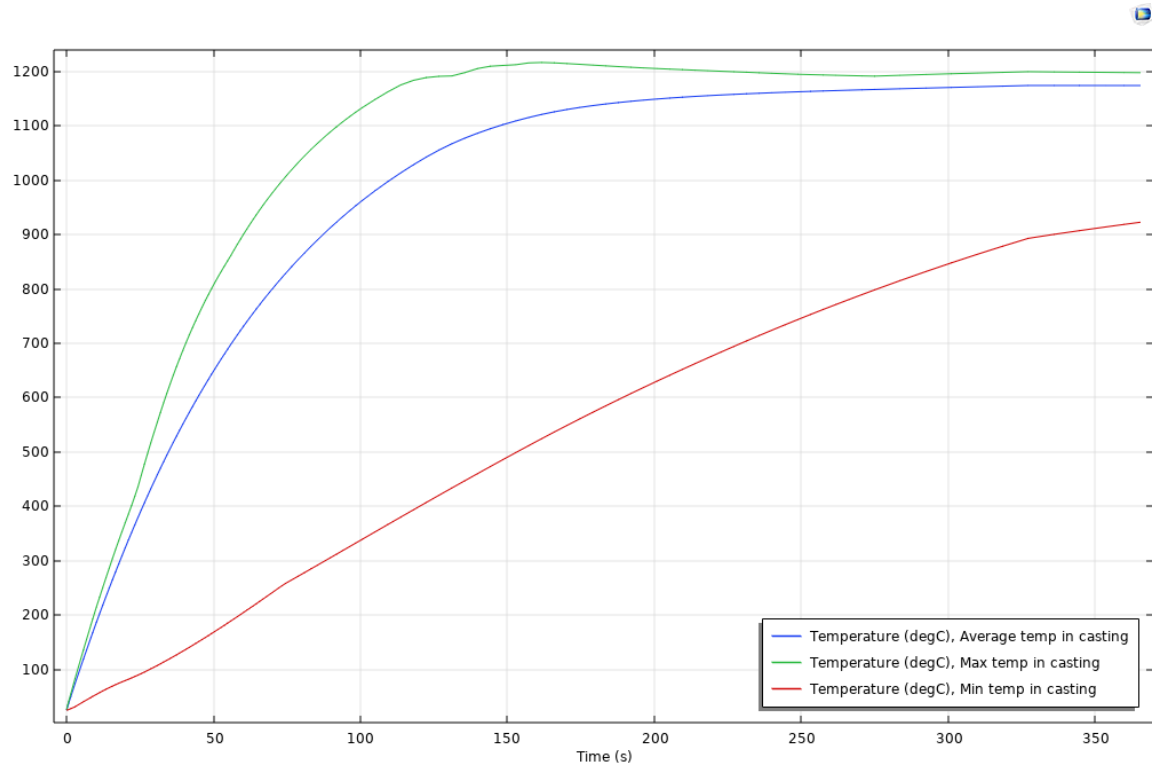

Figure 5: Average, maximum and minimum temperatures in the casting during the heating.

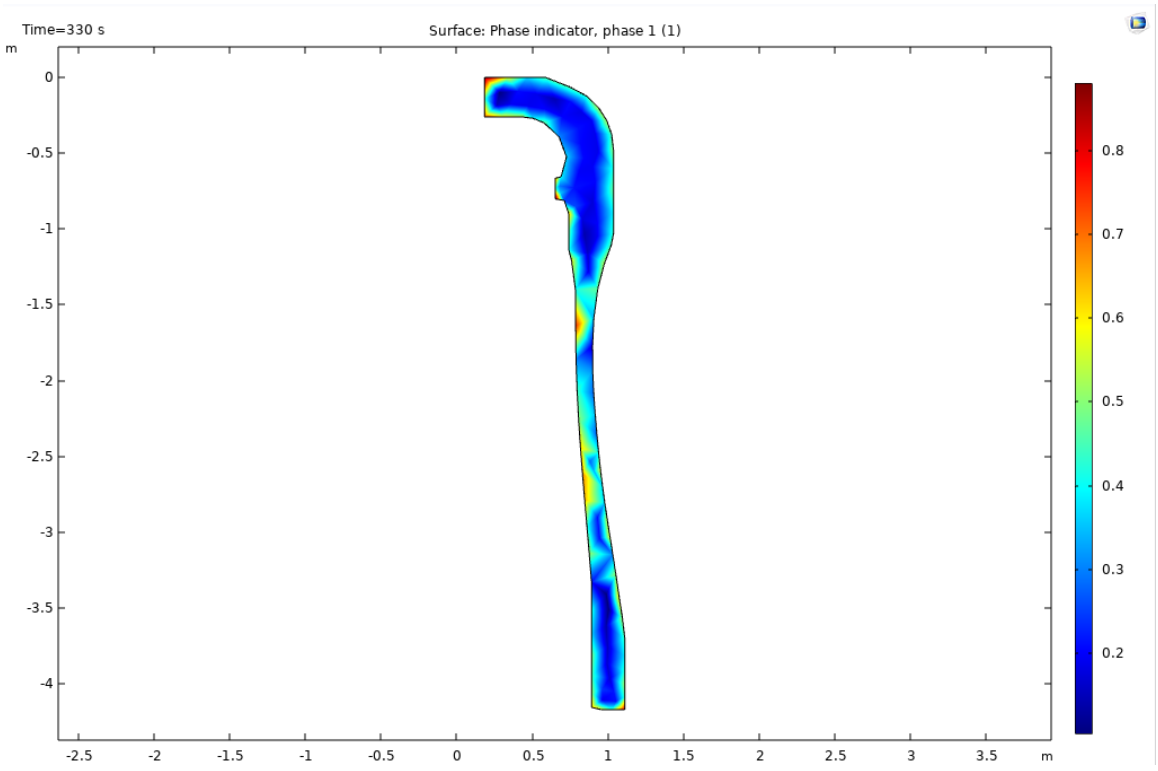

Figure 6: Solid phase indicator distribution in the casting at t=330 s.

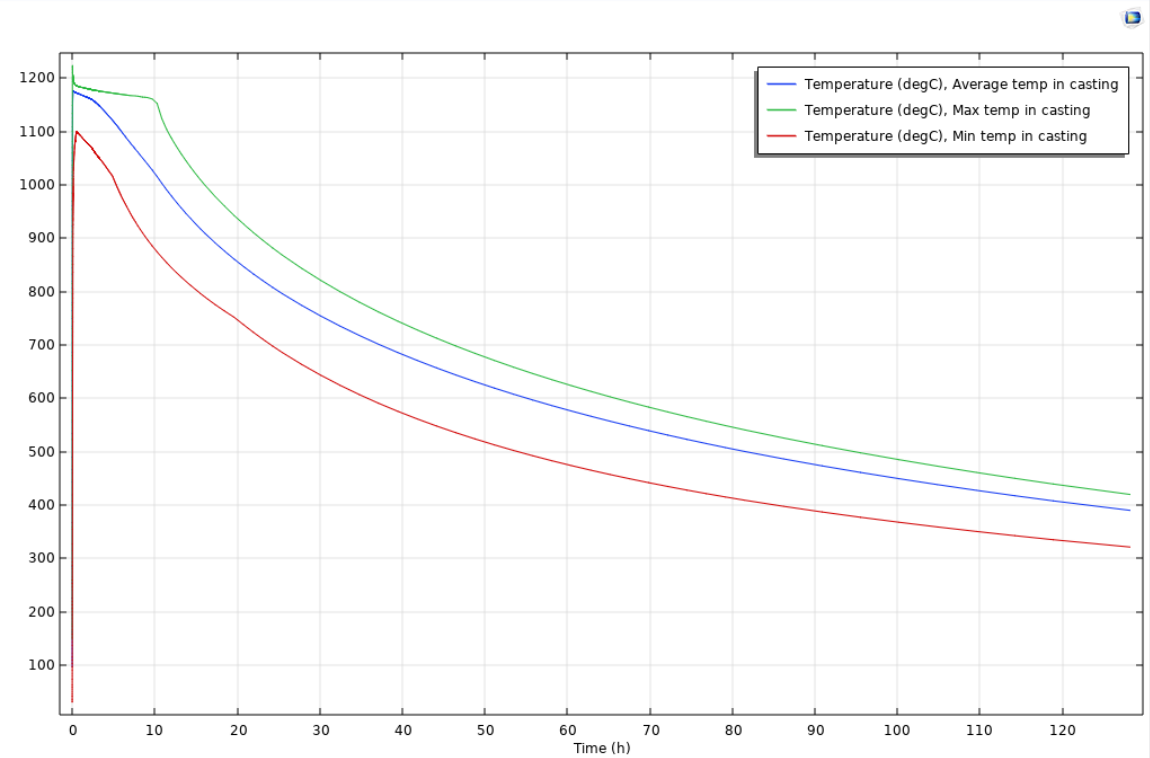

Figure 7: Average, maximum and minimum temperature in the casting product over five days in the current case simulation.

4.4 Current case

Figure 7 shows the average, maximum and minimum temperatures in the casting product from the start until t=120 h. The temperature profile at t=120 h in the current case is shown in figure 8a. The temperature span in the casting product at t=120 h is around 330-440 °C. Figure 8b shows the velocity magnitude in the air channel at t=120 h. All movement of air in the channel is caused by the natural convection and density changes due to Boussinesq's approximation.

However, the velocity profile in 8b is displayed with a inaccurate resolution. If the temperature and velocity profiles at one of the symmetry lines are displayed instead.

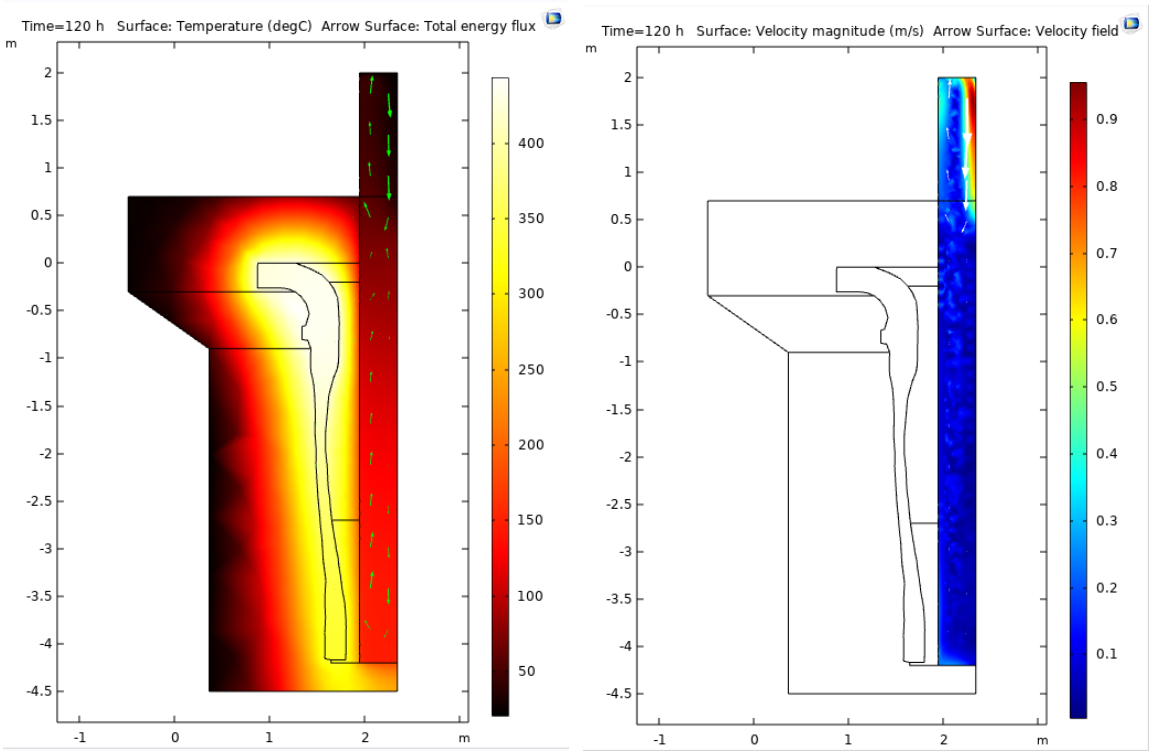

(a) Temperature profile. **(b)** Velocity profile.

Figure 8: Temperature and air velocity profiles for the current case simulation.

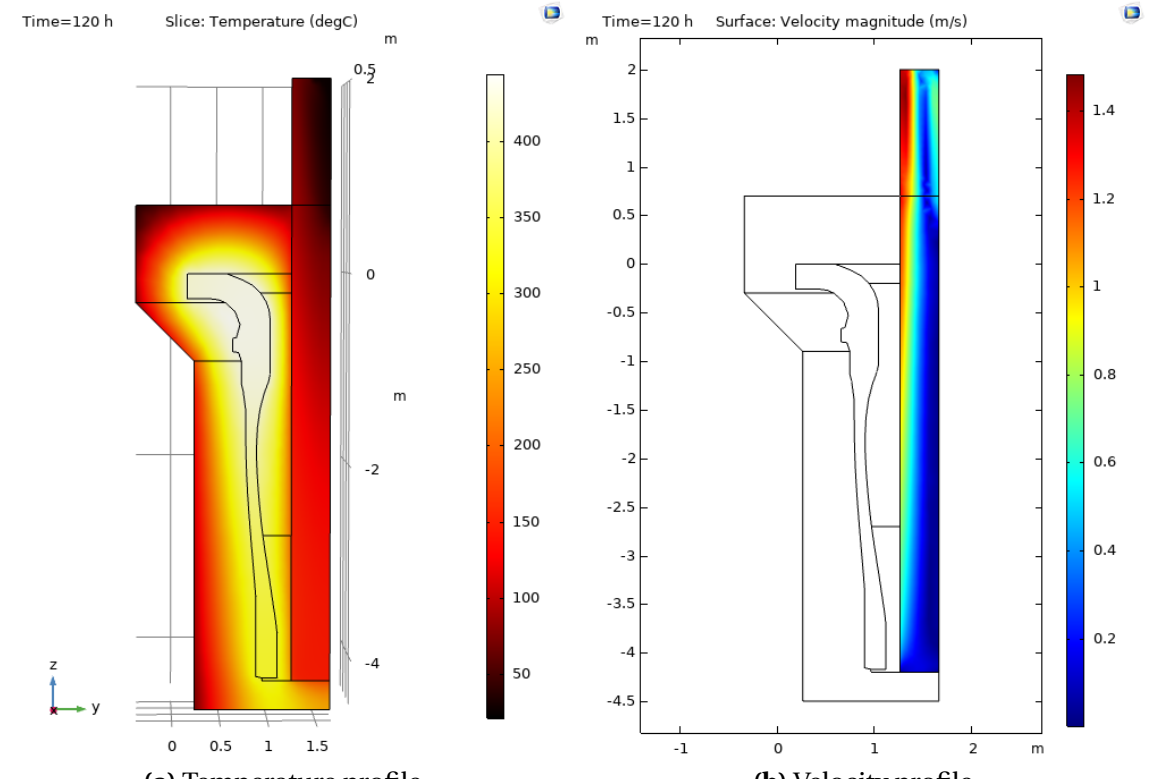

(a) Temperature profile. **(b)** Velocity profile.

Figure 9: Temperature and air velocity profiles at one of the symmetry lines for the current case simulation.

In Fig. 9b, it is shown that the velocity is at its highest close to the wall. This is due to the temperature dependent density, and the air close to the wall is heated more than the air in the middle of the channel.

4.5 Introducing forced convection

In this model, the air channel has been expanded and a forced air flow has been introduced through the channel. A couple of different inlet velocities have been tested. Figure 10 shows the temperature and air velocity profiles with the inlet velocity U_0 = 3 m/s at the top of the air channel. The maximum temperature in the model at t = 120 h is around 450 °C, and the velocity is completely dominant in the downwards direction. There is also a noticeable velocity boundary layer close to the wall. Figure 11 shows the average, maximum and minimum temperatures in the casting for the process. The temperature in the casting at t=120 h is in the interval 280-430 °C.

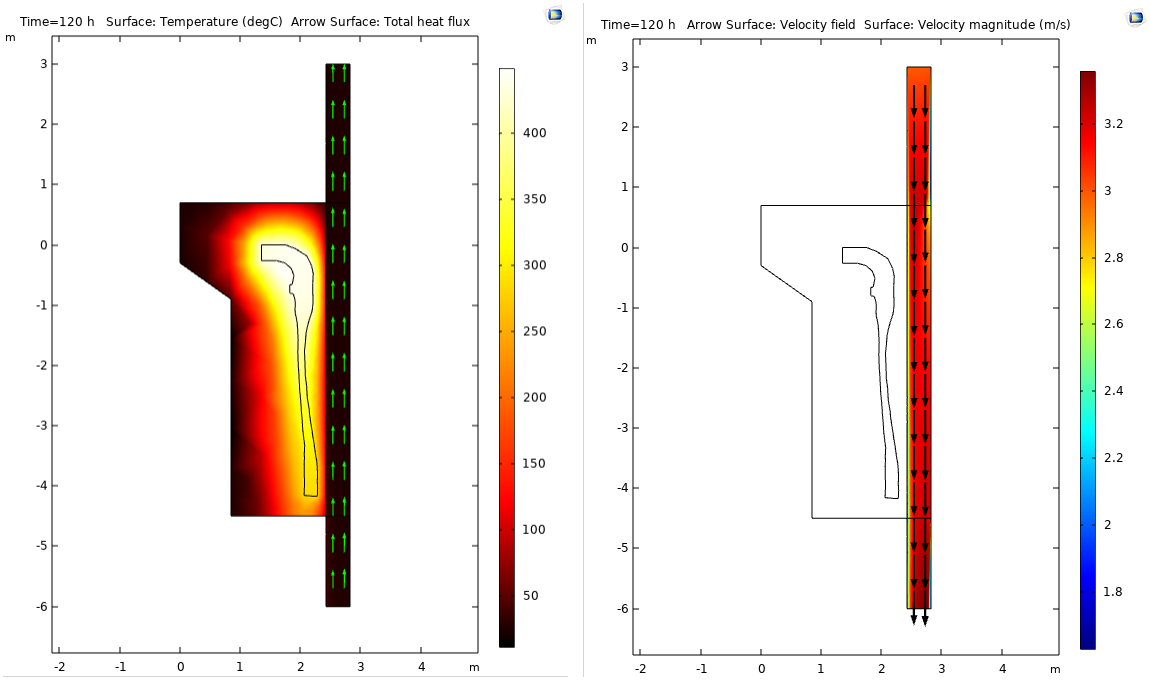

(a) Temperature profile. **(b)** Velocity profile.

Figure 10: Temperature and air velocity profiles for the simulation with a forced air flow with inlet velocity 3 m/s.

The air outlet mean temperature and the temperature profile at the air outlet are shown in figure 12. The mean outlet air temperature peaks at 35 °C at around t=20h. The horizontal temperature profile has a large temperature gradient quite close to the wall, and the temperature ranges between around 25 and 55 °C.

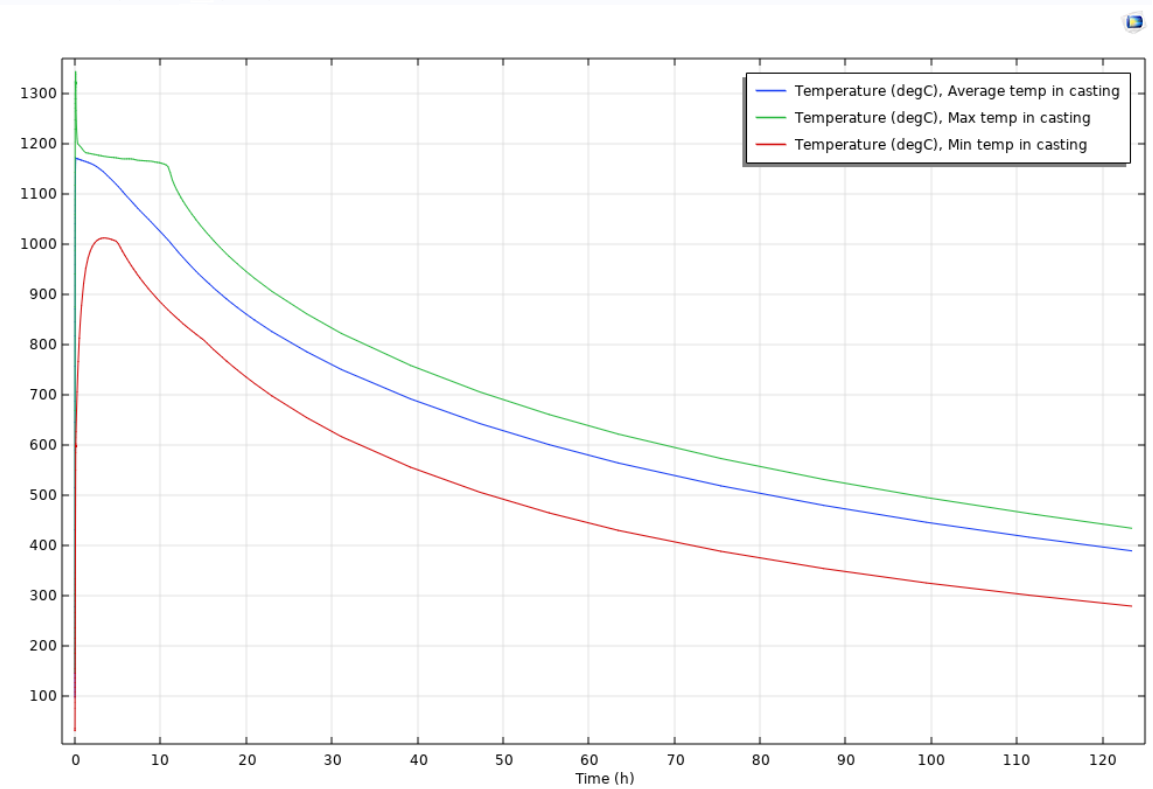

Figure 11: Average, maximum and minimum temperatures in the casting product over five days with a forced air flow (U_0=10 m/s).

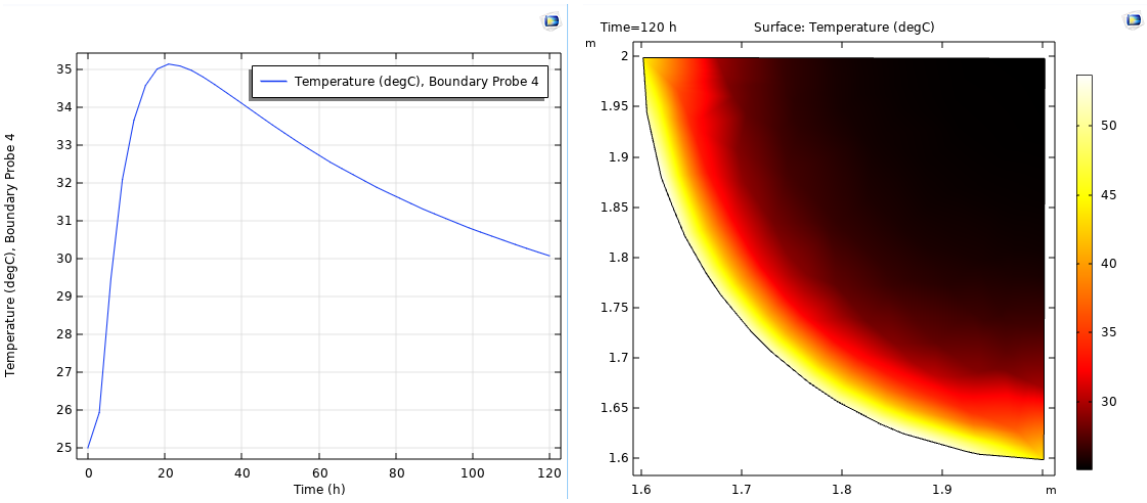

(a) Mean outlet temperature as a function of time. Each data point is updated every third hour.

(b) Horizontal temperature profile at the outlet at t=120 h.

Figure 12: Temperatures of the air outlet.

4.6 Introducing cooling fins

In this case, the sand form is equipped with eight cooling fins. The geomtry used to model the fins are shown in Figure 13. It is worth noting that the geometry used is somewhat arbitrary, and it is not optimized in any way for the process.

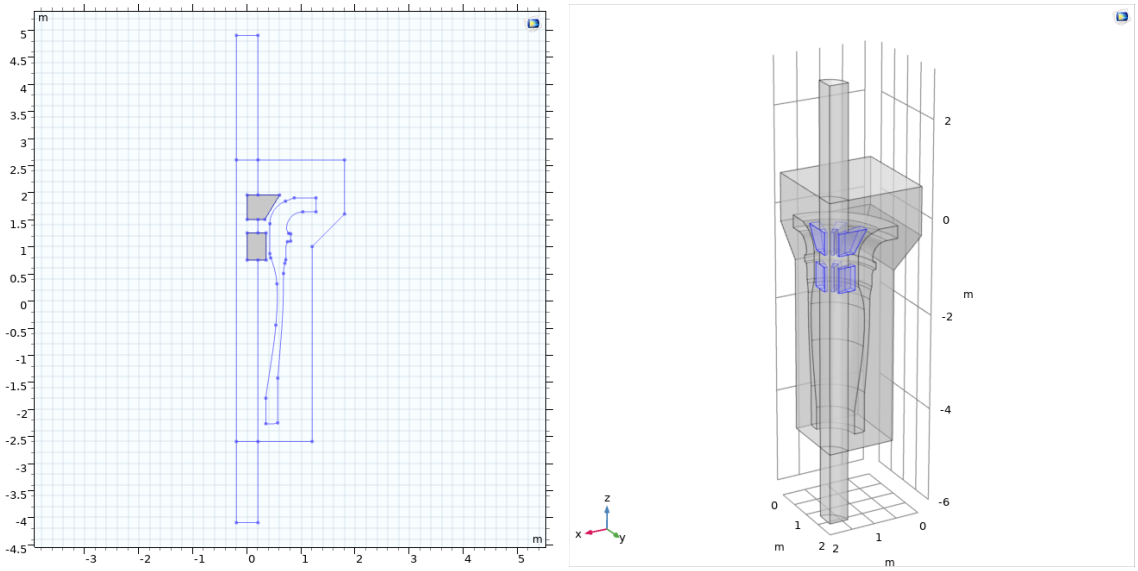

(a) 2D-geometry of the fins. **(b)** Geometry and location of the fins.

Figure 13: Geometry of the fins, and the 2D-geometry which is revolved into the 3D fins.

Ideally, the air movement should be modeled in the same way as in the current case, i.e., completely based on the natural convection due to density changes. However, this demanded too much computational time due to the increased number of mesh elements that occurred around the fins. Instead, the velocity profile in the model was used along with the temperature in the bottom of the air channel to mimic the behaviour of the air movement. This was modeled using the same geometric model as in section 4.5, i.e. with an extended air channel. U_0 was set to 0.1 m/s in the bottom of the channel. T_{inlet} was set to follow the air temperature in the bottom of the channel in the current case simulation. The data points as well as the interpolation between the points are shown in Figure 14.

The temperature and velocity profiles are shown in figure 15. The maximum temperature in the model is around 450 °C, and the velocity is dominant in the upwards direction. However, unlike in Fig. 8b, the velocity magnitude decreases close to the wall of the air channel.

The average, maximum and minimum temperatures in the casing over five days are shown in Fig. 16. The maximum temperature at t=120h is around 430 °C.

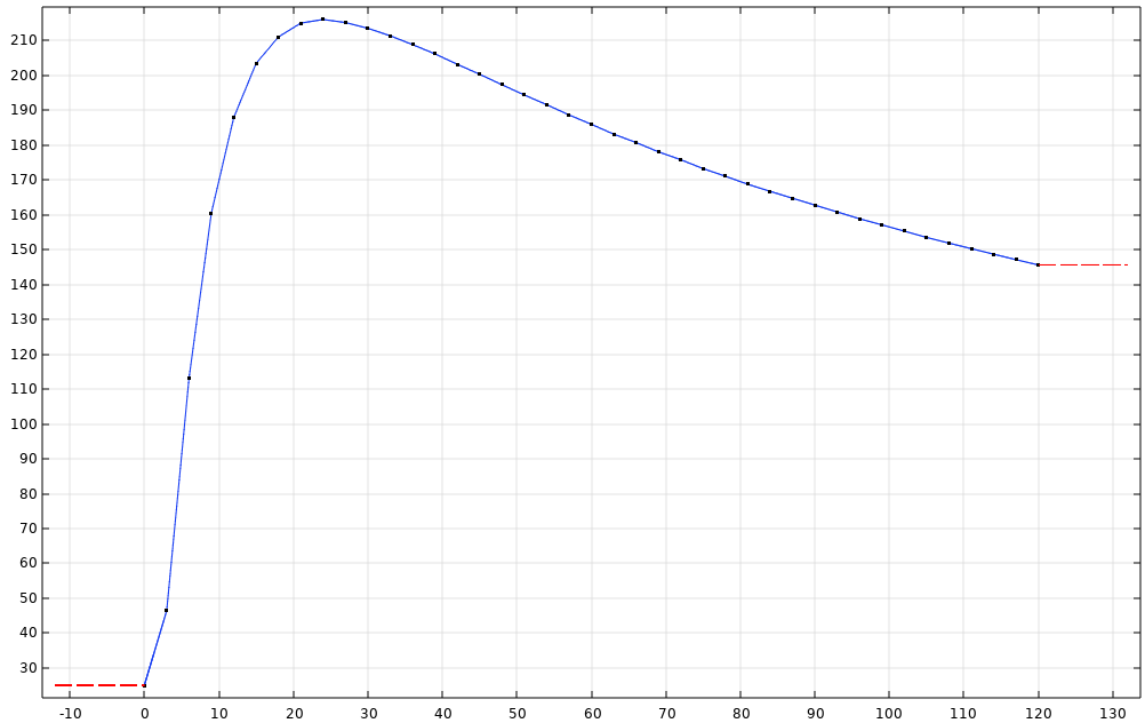

Figure 14: Model temperature used as T_{inlet} in °C as a function of time in hours for the simulation with added fins.

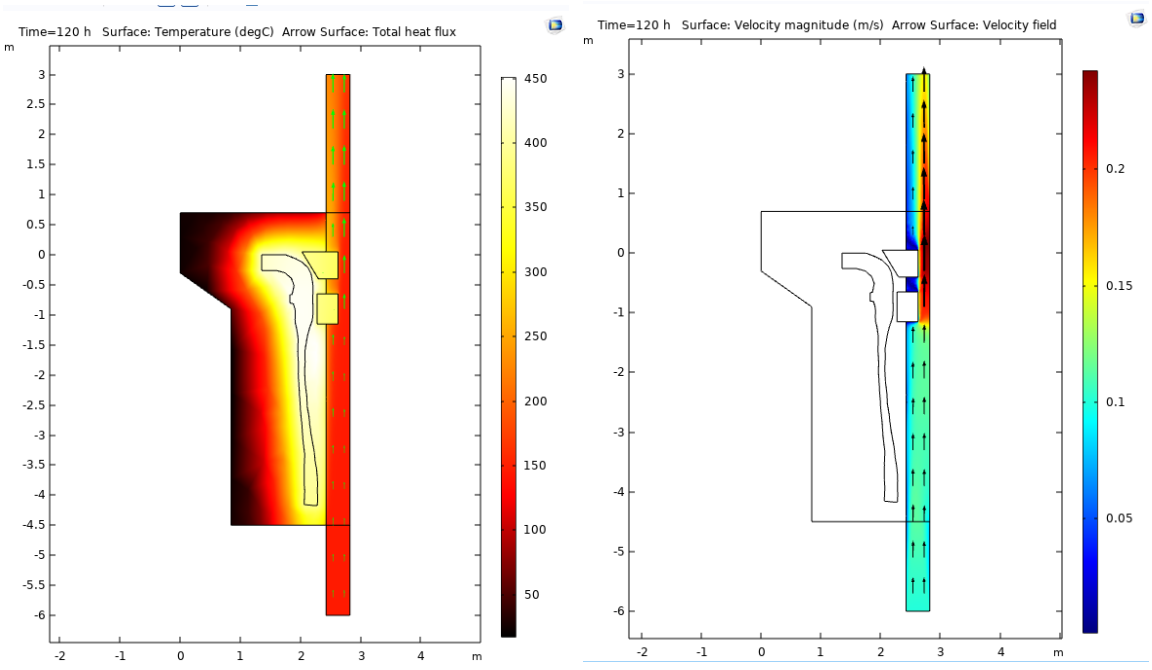

(a) Temperature profile. **(b)** Velocity profile.

Figure 15: Temperature and air velocity profiles for the simulation with fins and a forced air flow with U_0 = 0.1 m/s at t = 120 h.

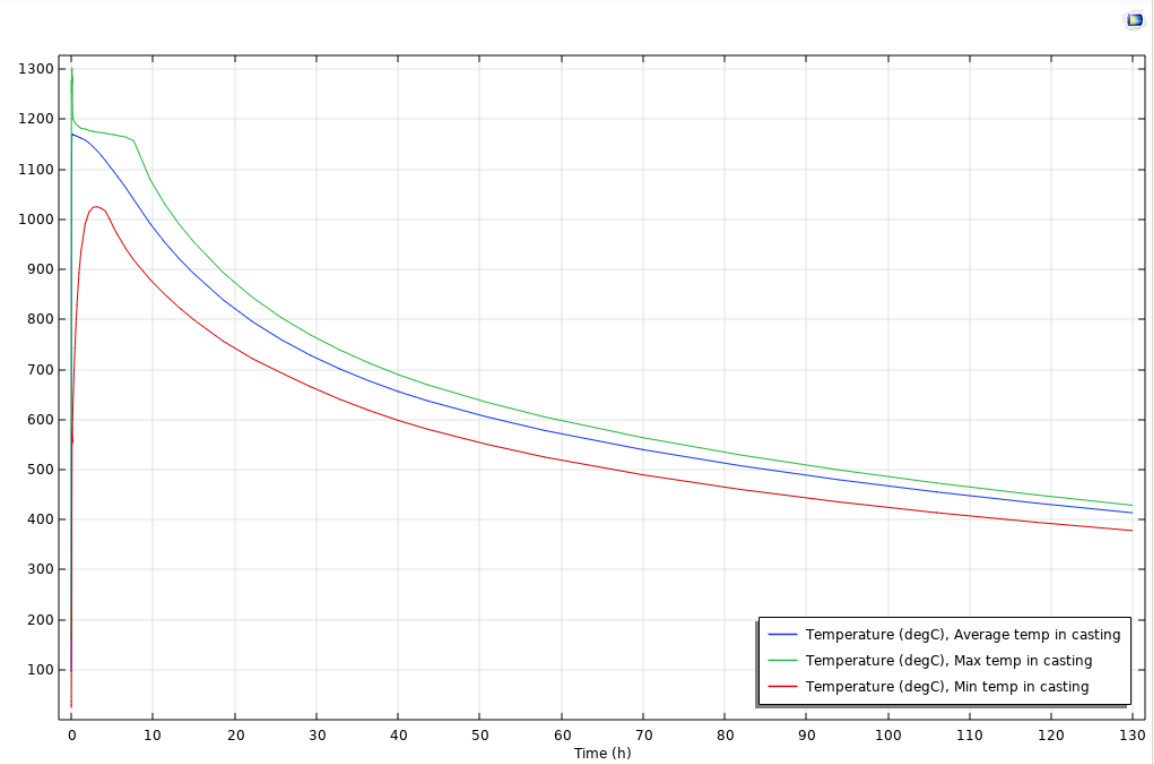

Figure 16: Average, maximum and minimum temperatures in the casting product over five days with a forced air flow (U_0=0.1 m/s).

4.7 Combining air flow and cooling fins

Finally, the two scenarios described in sections 4.5 and 4.6 are combined. The air inlet was placed at the top of the air channel, and a number of different values for U_0 was tested. Figure 17 shows the average, maximum and minimum temperatures in the casting during the process. The maximum temperature after five days is just over 300 °C, and T_{max} = 450 °C is reached at around t = 80 h.

Figure 18 shows the temperature and velocity profiles at t = 120 h.

Figure 19 shows the mean outlet temperature as a function of time and the horizontal temperature outlet at t=120h. The mean outlet air temperature peaks at just over 40 °C around t=18h, and at t=120 the mean output temperature is around 31 °C.

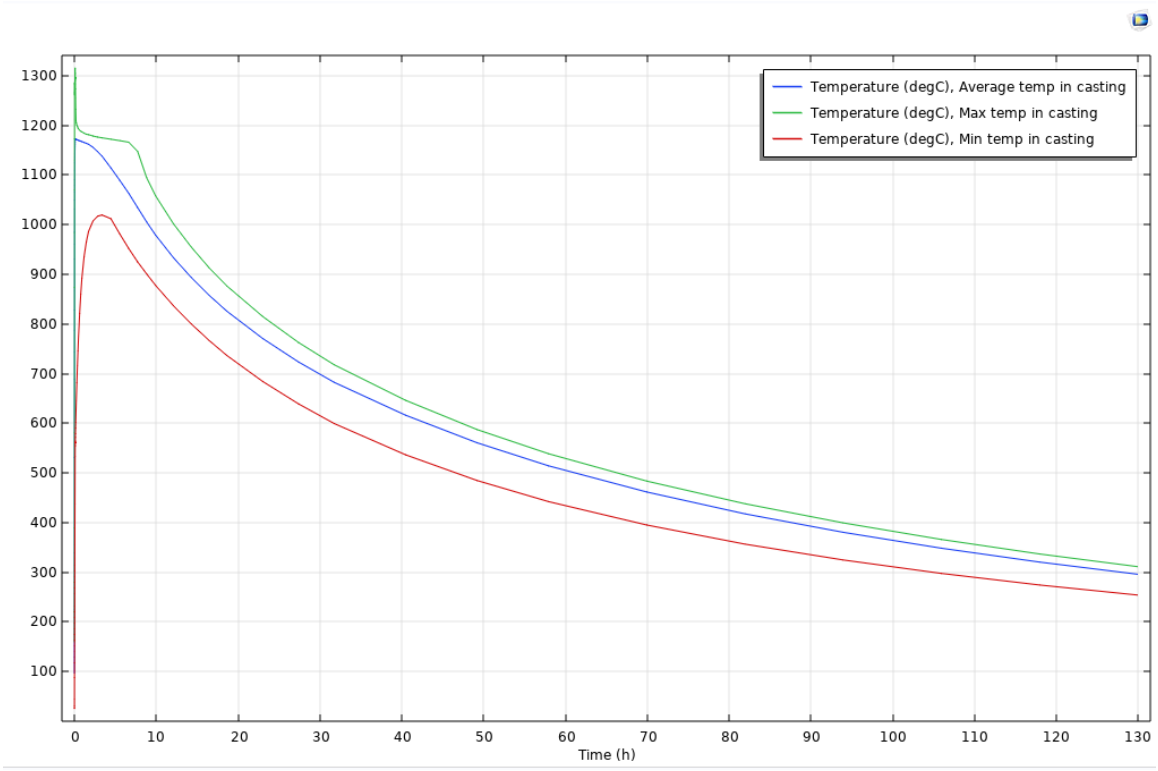

Figure 17: Average, maximum and minimum temperatures in the casting product over five days with both cooling fins and an air stream.

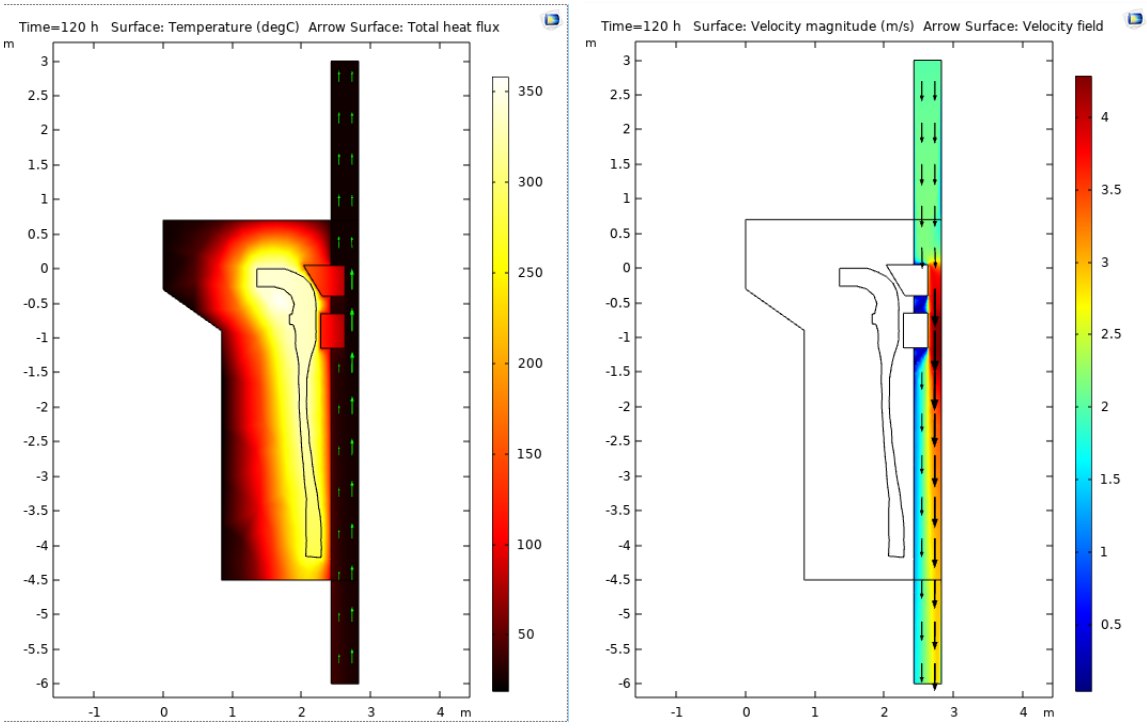

(a) Temperature profile. **(b)** Velocity profile.

Figure 18: Temperature and air velocity profiles for the simulation with both fins and a forced air flow with U_0 = 2 m/s at t = 120 h.

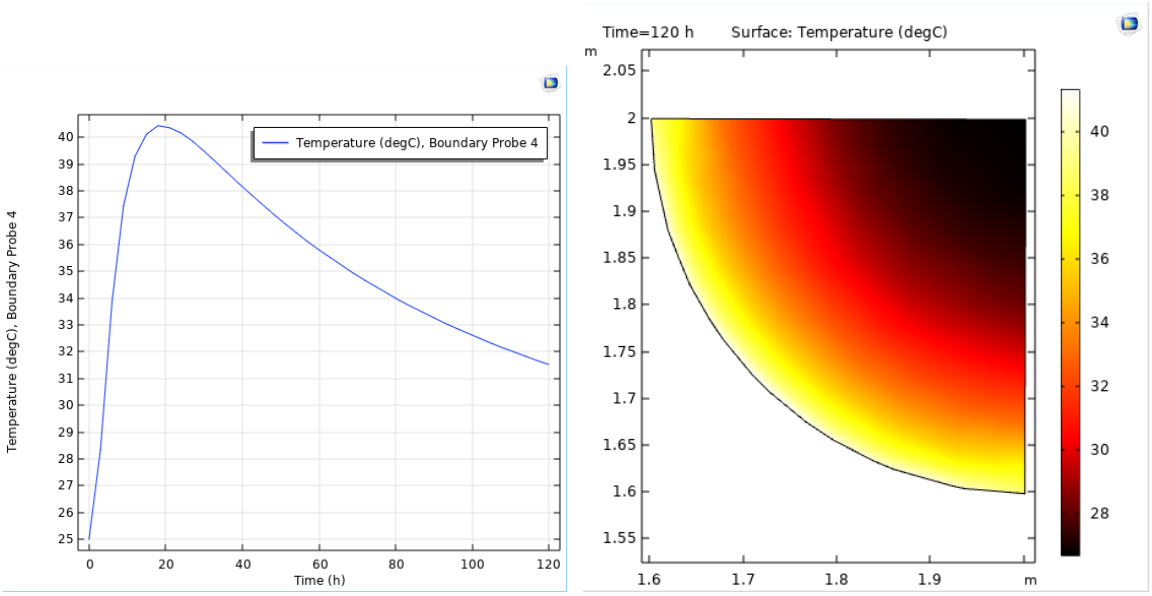

(a) Mean outlet temperature as a function of time. Each data point is updated every third hour. **(b)** Horizontal temperature profile at the outlet at t=120 h.

Figure 19: Temperatures of the air outlet.

The maximum and minimum temperatures in the casting after three, four and five days are shown in Table 5.

Table 5: Minimum and maximum temperatures in the casting after three, four and five days.

Simulated case	t = 72 h		t = 96 h		t = 120 h	
	T_{min}	T_{max}	T_{min}	T_{max}	T_{min}	T_{max}
Current case	435 °C	575 °C	380 °C	500 °C	335 °C	440 °C
Forced flow	400 °C	585°C	330 °C	505 °C	285 °C	440 °C
Fins	485 °C	560 °C	430 °C	495 °C	395 °C	445 °C
Fins & forced flow	390 °C	475 °C	320 °C	395 °C	270 °C	335 ° C

5 Analysis

5.1 Modeling the real application

5.1.1 Geometry changes

When modelling the real process, there were some issues with getting COMSOL to start the simulations. As mentioned in section 4.1.1 Geometry, some simplifications were performed on the CAD file provided from Valmet to solve this. This mainly concerned collapsing some chamfer and fillet faces into flat faces. This problem could possibly also have been solved by working with a finer mesh, but that would also increase the computational time. When the geometry is changed in this way, a consequence is that a change in volume implies a change in mass and therefore also in the heat distribution behavior. However, these changes in mass are very small compared to the rest of the casting, and should be considered negligible.

Another change in the geometry in the casting, which probably also is the most significant, is the neglecting of the cooling blocks. Even though the temperature profile for the current case matches the real application, the temperature change over time could possibly be different, with a steeper curve in the beginning. For this study, however, the behaviour was considered precise enough.

Lastly, the air channel is modeled with a diameter of 0.8 m, when it really is 1 m. The effects of this is that the sand layer between the casting and the air channel becomes thicker, which will decrease the heat transfer in that area. It also affects the air movement. A wider area makes the channel volume larger, which allows more movement due to natural convection. In the cases with a forced air flow, a wider air channel implies a larger air mass flux (assuming the inlet velocity U_0 is unchanged) and more air that will not touch the walls of the channel.

5.1.2 The heating module

As described in section 4.1.3 Initial values, and Eq. 19 in particular, the cast is heated during the first 330 seconds. Of course this is not how the real application works, but charging the form with heat in this manner was deemed to be interchangeable with just setting the initial temperature to 1200 °C. However, figure 5 shows that the average temperature in the casting reaches around 1170 °C. This temperature difference is small enough to be considered negligible for the results, especially since the total energy input is close to the theoretical heat that is added to the iron.

Figure 6 shows the distribution of liquid and solid iron in the end of the heating module. The scale does not reach either 0 or 1 in the ends, implying that no parts of the casting is fully liquid nor fully solid. The distribution also generally shows a higher solid phase indicator close to the edges of the casting. This is

because of the energy transferred to the surrounding sand due to the (initially) high temperature gradient. This phenomenon is also something that should be taken into consideration when comparing the liquid/solid-pattern to reality. In the real process, the iron in liquid state is poured into the form, and heat is immediately transferred to the sand as the form is filled. Since the iron in the model is heated rather than introduced as a liquid, the heating module will ”leak” heat to the surrounding sand. This means that even though the phase indicator plot shows that not all the iron is in liquid state, which could be used as an argument against the models credibility, the energy added during the heating could possibly represent the heat added by pouring 23 tonnes of liquid iron into the form. This is also why the integration of the heating module output was considered when determining the parameters.

5.2 Choice of governing equations and boundary conditions

5.2.1 The solidification and cooling process

As shown in Figure 7, the maximum temperature at t=120 is just under 440 °C. This is lower than in the real process, but was assumed to be close enough to use as a reference model for the altered cases.

5.3 Current case simulation

The current case simulation was the one on which undoubtedly most time was spent, as the meaning of that simulation has been to act as a reference for the other cases. Fig 8b is the only velocity profile that has its boundary layer turned that way, i.e, a higher velocity closer to the wall. This is a direct consequence of the fact that natural convection is the only driving force for the air movement. However, the air velocity magnitude is close to 0 except in the very top of the air cylinder.

5.4 Introducing an air stream

As seen in figure 10a, the temperature boundary layer is following the same pattern as the current case. Since new, cool air is introduced into the air channel, the temperature gradient towards the center is larger. However, this seems to mainly affect the coldest part of the casting, based on Fig. 11. The temperature gradient in space increases, which if too large could lead to breakings in the material. Since the warmest part in the casting is about the same temperature as in the current case simulation, this seems to be quite inefficient as a cooling method. As seen in Fig. 12, most of the air is not heated very much, and the mean outlet temperature is overall quite low. This is most likely due to the size of the air channel. When the air flows into the channel, it is not mixed due to the width of

the channel. Therefore, most of the air just passes by without being heated since there is only a thin layer that touches the walls.

5.5 Introducing fins

Modeling the introduction of the fins was a bit problematic, since the modeling of natural convection using the Boussinesq approximation demanded too much computational time. The effect of ”mimicking” the behaviour is shown in figure 15, when looking at the velocity boundary layer close to the wall. The boundary layer is increasing in the opposite direction compared with the current case, even though the velocity is very low. Since the density is modeled as a constant, the only driving force is the air inlet velocity and the continuity of the air movement. The non-moving air close to the wall is also affecting the temperature profile. Since it is practically standing still, it creates an isolating layer at the wall, which in turn evens out the temperature gradient in the sand. A smaller temperature gradient in space, i.e., ∇T, affects Eq. 3 and therefore slows down the cooling process. This is probably the reason why the maximum temperature in the casting at t=120h is higher than in the current case simulation.

5.6 Introducing both fins and an air stream

When both the fins and an air stream was introduced to the model, the temperature in the casting is drastically lowered according to Fig. 18a. The increase in heat leaving the form is also connected to Fig. 19; the mean outlet temperature is higher than with just the air flow, and the temperature profile is slightly more distributed. This is probably due to the fins in two ways. Firstly, the fins increase the conductive heat flux inside the form from the casting to the air channel. Secondly, the fins also cause a mixing in the channel, which letmore air to be in contact with the walls. The cooling air in turn works as a ”cool sink” for the fins, keeping ∇T up in Eq. 3. In Fig. 18b there is a ”pocket” with very low velocity between the two fins. This could have a negative effect of the cooling. However, there are no direct effects visible in the temperature distribution in Fig. 18a alone. The temperature plot in Fig. 17 shows that the temperature in the casting varies between about 250 and 310 °C, which is a more narrow interval than in the current case simulation.

6 Discussion

6.1 Models and simulations compared to reality

A number of differences between the geometry used in the model and the actual form has been listed and evaluated. In order to get a more representative model, the cooling blocks and the iron ”skeleton” should be included. Even if the sand form contains a lot of different components that has not been brought up in the report, these should not matter too much for the heat transfer process, since they do not make up a remarkable large fraction of the materials in the form. However, simulating the process with the sand saving iron pipe between the sand and the air channel would probably affect the process in mainly two ways. Firstly, another material layer would be added in the main direction of the conductive heat transfer, affecting the heat transfer rate from the casting form to the air. Secondly, since the iron has a significantly higher thermal conductivity than sand, it would probably increase the heat transfer rate along with the channel. This would implies a more even wall temperature. However, it is hard to make any definite conclusions for that effect, since there are a lot of other factors affecting the heat transfer.

The results from the simulations would probably be different if the air channel was to be modeled with the correct diameter. It is hard to draw any conclusions regarding how any of the cases would be affected, more than the forced airflow would pump in even more air that would not contribute to the cooling. However, if a ”turbulence enhancing” geometry is introduced to the channel, the air could probably be heated more efficiently than in the simulated cases.

The cooling fins used in the modified models are not optimized in any way, i.e., there have not been any comparisons in how different geometries, number of fins or placement would affect the velocity or temperature profiles. Also, it is hard to draw any conclusions from the simulations where just the cooling fins were introduced since the effects of the natural convection has not been properly examined.

From the simulations, the model with both fins and a forced air flow was by far the most efficient when it came to cooling the casting. If this should be introduced to the real application, the fins would probably be the easiest part as they could be build onto the sand saving iron pipe. The air stream could be harder to implement, since the design of the current sand form would need to be changed a lot. A solution in how to connect the sand form to both an inlet and an outlet for the air also needs to be developed. If the excess heat from the air stream should be reused in some way, a solution to take care of that heat also has to be developed.

In terms of energy efficiency, the study has not covered the energy needed to produce an air stream used in the simulations. The effects of different velocities of the input air are also not covered by the study, but that could change the results. In all simulations that have been done during the project, the inlet

velocity has been set as a constant. It is possible that as the temperature lowers throughout the process, the cooling need could be achieved by a smaller mass flow. This would probably increase the output temperature, and in turn change the possibilities for reusing the heat.

6.2 Using COMSOL Multiphysics

If only the casting procedure was to be simulated and evaluated, there are other software products that the industries already use. However, one of the biggest advantages of using COMSOL Multiphysics for this type of simulations is probably the possibilities to couple different physical concepts to each other. It is relatively easy to connect the heat and mass transfer phenomena, and working in a 3D environment, where it is possible to import external CAD files, makes it very user friendly.

The backside is that using a program like this demands a lot of knowledge about the theory behind the physics, and how to build an efficient model. During the project, a lot of time has been spent on troubleshooting the model because the simulations would not start, or took unreasonably long time. Of course this is mainly a question about learning the program, what works and what does not.

In order to get the most out of COMSOL Multiphysics, the user also has to know how to build an efficient mesh. It should be detailed enough to represent the geometry of the casting and the components, but if it is too detailed the calculations could be to extensive to be performed in a reasonable amount of time. The difficulty of building the mesh is also affected by the complexity of the geometry itself, and the more details there is in a model the harder it could be to build an effective mesh.

6.3 About the method

This project has been very component focused, and a lot of time has been invested in building, modifying and evaluating the model. The project would have been improved by putting more time into looking more deeply into material properties, and how to model the sand form. It would also have given a lot to the results to make some kind of thermoeconomic analysis, i.e., investigating the value of taking care of the excess energy.

Regarding the simplifications of the model, both in terms of simplifying the CAD file and excluding some parts in the form, it should still be sufficient as a pointer in how the process could be modified.

7 Conclusions

7.1 What would work?

In order to decrease the required cooling time for the model in question, an efficient way would be to both increase the conductive heat transfer in the sand form and introducing a cooling air stream. Fins would probably be quite easy to introduce in the process as they can be built onto present components. However, the geometry of the fins has not been evaluated enough to say what an optimized setup would look like. There is also no clear way in how to introduce the air stream in the process, or complications in combining such a setup with the current process.

7.2 Using COMSOL

COMSOL Multiphysics works fairly well to simulate the type of processes that this project has been about, especially when evaluating not only the casting but also the surroundings and combining different processes. It does however require a lot of theoretical knowledge about all those processes.

8 Recommendations & future work

Before any of the ideas presented in this report can be used in a real process, a couple of different things have to be studied as well.

Fin optimization

The geometry, placement and amount of fins should be further investigated to get an optimized heat transfer process.

Implementation of the air stream

The forced air stream is very efficient in theory, but before it can be used in the real process the possibilities to actually implement the components needs to be investigated. Also, the effect of different air velocities should be further investigated to optimize the process.

Recycling of the heat

Even if the cooling time is reduced with the implementations investigated during this project, the possibilities to reuse the excess heat is something that should be further investigated. Apart from the changes in energy demand, a thermoeconomic analysis should be performed to find out what the costs of investing in such a system could be, and also if there are any economic savings achievable when implementing such a system.

Appendices

A Material properties for cast iron

Table 6: Conductivity for the cast iron, provided by RISE Swecast.

Temp (C)	Conductivity (W/m/K)
47	20.8813
77	21.0544
107	21.2303
137	21.4092
167	21.5911
197	21.7761
227	21.9644
257	22.1559
287	22.3508
317	22.5491
347	22.7510
377	22.9566
407	23.1659
437	23.3790
467	23.5962
497	23.8173
527	24.0427
557	24.2724
587	24.5065
617	24.7451
647	24.9885
677	25.2367
707	25.4899
737	25.7482
767	26.0117
797	26.2808
827	26.5555
857	26.8359
887	27.1224
917	27.4150
947	27.7140
977	28.0196
1007	28.3321
1037	28.6516
1067	28.9783
1097	29.3126
1127	29.6547
1139	29.7163
1142	29.7227
⋮	⋮
1145	29.7105
1148	29.6615
1151	29.5332
1154	29.2226
1157	28.4994
1160	27.4891
1163	27.4912
1166	27.4931
1169	27.4947
1172	27.4962
1175	27.4974
1178	27.4983
1181	27.4990
1184	27.4995
1187	27.4996
1190	27.4995
1193	27.4992
1196	27.4985
1199	27.4975
1202	27.4968
1205	27.5520
1209	27.6256
1239	28.1773
1269	28.7288
1299	29.2799
1329	29.8307
1359	30.3813
1389	30.9315
1419	31.4815
1449	32.0311
1479	32.5805
1509	33.1296
1539	33.6784
1569	34.2269
1599	34.7751
1629	35.3230
1659	35.8706
1689	36.4180

Table 7: Enthalpy for the cast iron, provided by RISE Swecast.

Temp (C)	Enthalpy (kJ/kg)
47	146.06
77	160.225
107	174.692
137	189.435
167	204.433
197	219.669
227	235.128
257	250.799
287	266.671
317	282.737
347	298.989
377	315.420
407	332.027
437	348.803
467	365.745
497	382.850
527	400.115
557	417.537
587	435.114
617	452.844
647	470.726
677	488.757
707	506.937
737	525.264
767	543.737
797	562.357
827	581.121
857	600.029
887	619.080
917	638.275
947	657.613
977	677.092
1007	696.714
1037	716.478
1067	736.383
1097	756.430
1127	776.618
1139	790.878
1142	794.723
1145	800.079

Temp (C)	Conductivity (W/m/K)
⋮	⋮
1148	808.465
1151	823.380
1154	853.202
1157	916.371
1160	1002.36
1163	1006.91
1166	1011.50
1169	1016.14
1172	1020.83
1175	1025.57
1178	1030.36
1181	1035.21
1184	1040.11
1187	1045.07
1190	1050.08
1193	1055.16
1196	1060.29
1199	1065.49
1202	1070.71
1205	1072.94
1209	1075.93
1239	1098.45
1269	1121.26
1299	1144.34
1329	1167.71
1359	1191.39
1389	1215.39
1419	1239.73
1449	1264.42
1479	1289.48
1509	1314.94
1539	1340.80
1569	1366.87
1599	1392.94
1629	1419.02
1659	1445.10
1689	1471.19

B Heat source calculation

Table 8: Heat source output for the heating of the iron initially in the simulations.

Time (s)	Heat source output (kW)
0	28686
0.36	57090
0.72	56812
1.44	56262
2.88	55184
5.76	53129
8.27	51389
8.90	50959
10.15	50114
11.23	49392
12.32	48680
13.41	47977
14.51	47284
15.59	46598
16.68	45921
17.77	45253
18.86	44592
19.95	43939
21.04	43295
22.13	4266
23.22	42034
24.31	41416
25.40	40808
26.49	40209
27.58	39619
28.67	39037
29.76	38465
30.85	37901
31.94	37346
33.03	36800
34.12	36261
35.21	35732
36.30	3521
37.39	34696
38.48	34191
39.57	33693
40.66	33203
41.75	32720
42.84	32245
43.93	31777
45.02	31316
46.11	30863
47.20	30416
48.29	29976
49.38	29543
50.47	29117
51.56	28697
52.65	28284
53.74	27876
54.83	27476
55.92	27081
57.01	26692
58.10	26309
59.19	25932
60.28	25561
61.37	25195
62.46	24835
63.55	24481
64.64	24132
65.73	23788
66.82	23449
67.91	23115
70.09	22468
⋮	⋮
72.27	21839
74.45	21229
76.63	20638
78.81	20063
80.99	19506
83.17	18965
85.35	18440
87.53	17930
89.71	17435
91.89	16955
94.07	16488
96.25	16035
98.43	15596
100.61	15169
104.97	14362
109.33	13601
113.69	12882
118.05	12205
122.41	11570
126.77	10987
131.13	10465
135.49	10005
139.85	9594
144.21	9220
148.57	8880
152.93	8572
157.29	8290
161.65	8039
166.01	7818
170.37	7624
174.73	7455
179.08	7305
183.44	7172
187.8	7052
192.16	6945
196.52	6848
200.88	6761
205.24	6681
209.6	6608
213.96	6542
218.32	6481
222.68	6426
227.04	6374
231.4	6326
235.76	6281
240.12	6239
244.48	6199
248.84	6161
253.2	6126
257.56	6091
261.92	6059
266.278	6028
270.64	5997
275	5967
283.72	5910
292.44	5855
301.16	5800
309.88	5747
318.60	5693
327.32	5639
336	0

References

Askeland, Donald R. and Wendelin J. Wright (2017). *Essentials of Materials Science and Engineering*. 4th ed. Boston, Massachusetts: Cengage Learning. ISBN: 9781337629157.

Bannach, Nancy (2014). *Phase Change: Cooling and Solidification of Metal*. COMSOL. URL: https://www.comsol.com/blogs/phase-change-cooling-solidification-metal/ (visited on 03/07/2019).

COMSOL (2018a). *CFD User's Guide*. Documentation for COMSOL Multiphysics 5.4. Part number: CM021301.

COMSOL (2018b). *COMSOL Multiphysics - Reference manual*. Documentation for COMSOL Multiphysics 5.4. Part number: CM020005.

COMSOL (2018c). *Heat Transfer Module User's Guide*. Documentation for COMSOL Multiphysics 5.4. Part number: CM020801.

Energimyndigheten (2017). *Energiläget 2017*. Report. ISSN: 1404-3343. Statens energimyndighet.

Farre, Sten (2012). *Värmeledning i sandform*. 2012-007. Swerea Swecast. (Visited on 12/18/2018).

Fontes, Ed (2016). *Introduction to Modeling Natural Convection in COMSOL Multiphysics®*. COMSOL. URL: https://www.comsol.com/blogs/introduction-to-modeling-natural-convection-in-comsol-multiphysics/ (visited on 03/03/2019).

Frei, Walter (2017). *Which Turbulence Model Should I Choose for My CFD Application?* COMSOL. URL: https://www.comsol.com/blogs/which-turbulence-model-should-choose-cfd-application/ (visited on 02/28/2019).

Gothäll, Hanna (2017). *How to Inspect Your Mesh in COMSOL Multiphysics*. COMSOL. URL: https://www.comsol.com/blogs/how-to-inspect-your-mesh-in-comsol-multiphysics/ (visited on 03/13/2019).

Nilsson, Bernt (2017). *Applied Transport Phenomena - Lecture notes (Draft 2017A)*. Unpublished material.

Spakovszky, Z. S. (2007). *Thermodynamics and Propulsion*. MIT. URL: http://web.mit.edu/16.unified/www/FALL/thermodynamics/notes/node18.html (visited on 01/09/2019).

Sundén, Bengt (2012). *Introduction to Heat Transfer*. Boston, Massachusetts: WIT Press. ISBN: 1845646568.